UCLA Structural / Earthquake Engineering
Research Laboratory

ASSESSMENT OF 2015 AND 2018 E-DEFENSE 10-STORY REINFORCED CONCRETE BUILDINGS BASED ON ACI 318 AND ASCE 7 PROVISIONS

Final Report

Mehmet E. Unal
Kristijan Kolozvari
John W. Wallace

University of California, Los Angeles
California State University
Department of Civil & Environmental Engineering

Koichi Kajiwara, Jae-Do Kang, Yusuke Tosauchi,
Eiji Sato, Toshimi Kabeyasawa, Hitoshi Shiohara,
Takuya Nagae, Toshikazu Kabeyasawa

E-Defense and Japanese Researchers

Report to the American Concrete Institute Foundation

Henry Samueli School of Engineering and Applied Science
University of California, Los Angeles

December 2021

UCLA SEERL
2021/01
December 2021

ASSESSMENT OF 2015 AND 2018 E-DEFENSE 10-STORY REINFORCED CONCRETE BUILDINGS BASED ON ACI 318 AND ASCE 7 PROVISIONS

Final Report

Mehmet E. Unal
Kristijan Kolozvari
John W. Wallace

University of California, Los Angeles
California State University
Department of Civil & Environmental Engineering

Koichi Kajiwara, Jae-Do Kang, Yusuke Tosauchi,
Eiji Sato, Toshimi Kabeyasawa, Hitoshi Shiohara,
Takuya Nagae, Toshikazu Kabeyasawa

E-Defense and Japanese Researchers

Report to the American Concrete Institute Foundation

Henry Samueli School of Engineering and Applied Science
University of California, Los Angeles

December 2021

ABSTRACT

The E-Defense shake table facility, the world's largest three dimensional (3D) full-scale earthquake testing facility, was constructed by National Research Institute for Earth Science and Disaster Resilience (NIED) in 2005 in Miki, Japan. Since then, over 80 full-scale or large-scale experiments are conducted to have a better understanding of the effects of earthquakes on structures. In December 2015 and later in December 2018 and January 2019, NIED tested two 10-story reinforced concrete (RC) buildings on the E-Defense shake table. The main purpose of this report is to evaluate these buildings using the current provisions of ACI 318 (2019) and ASCE 7 (2017), and to gain better knowledge on the effectiveness and accuracy of these standards. The lateral force resisting systems for the buildings consisted of special reinforced concrete shear walls (bearing wall systems) in one direction and special reinforced concrete moment frames (moment-resisting frame systems) in the orthogonal direction. Three-dimensional elastic models are created using the structural engineering software ETABS® 2018. Model results showed that, for 2015 test structure, beam and columns shear reinforcement and transverse reinforcement for special boundary elements (SBEs) were modestly less than required by ACI 318-19 provisions. Although diagonal shear cracks were reported within some beam-column joints after the 2015 experiment, current provisions of ASCE 41-17 were not able to predict these joint shear failures, although more detailed approaches proposed in the literature suggested joint damage might occur. For 2018 building, joint and column transverse reinforcement and column-to-beam strength ratios were increased such that they satisfied ACI 318-19 provisions; however, special boundary elements transverse reinforcement and beam shear reinforcement near beam ends still were modestly less than required by ACI 318-19.

ACKNOWLEDGEMENTS

The work presented in this report was supported by funding from the American Concrete Institute Foundation Project CRC 2020 P0038. This financial support is gratefully acknowledged. This report should provide details associated with these tests that enable future studies, such as reported in journal papers published by the authors and others in a Special Issue of the Bulletin of Earthquake Engineering - International Joint Research on the Ten-story RC Full-scale Buildings Tested at E-Defense Shaking Table. The support of our Japanese co-authors in obtaining information and clarifications related to test details is gratefully acknowledged. Any opinions, findings, and conclusions or recommendations expressed in this report are those of the authors and do not necessarily reflect the views of the ACI Foundation or other individuals or groups mentioned here.

TABLE OF CONTENTS

LIST OF FIGURES

LIST OF TABLES

CHAPTER 1. INTRODUCTION AND ORGANIZATION

1.1 Introduction

Construction of world's largest shaking table facility (E-Defense) in Miki, Japan was undertaken in 1999 and completed in 2005 (10 years after Kobe Earthquake) by National Research Institute for Earth Science and Disaster Resilience (NIED). Since being commissioned, the E-Defense facility has provided the civil engineering community around the world to study the behavior of large- and full-scale structures subjected to strong ground shaking. First in December 2015 and later in December 2018 and January 2019, as part of its "Social Infrastructure Research Utilizing the 3D Full-Scale Earthquake Testing Facility" project, NIED conducted several shaking table tests on 10-story reinforced concrete buildings to better understand failure mechanisms of full-scale structures during earthquakes and to verify the effects of seismic retrofitting [4]. During the testing, buildings were subjected to increasing intensity shaking using JMA Kobe and Takatori recorded ground motion records.

The main objective of this report is to summarize results from an investigation to assess the degree to which these test buildings satisfy the design requirements of ASCE 7-16 and ACI 318-19. To this end, 3D elastic models of the buildings are created using the computer software ETABS®, and member demands and lateral drifts were calculated using the ASCE 7-16 Modal Response Spectrum Analysis procedure using a Risk-Targeted Maximum Considered Earthquake (MCE_R) spectrum that reasonably represents the demands imposed by the Kobe JMA record scaled to 100%, reduced to 2/3 to represent design earthquake shaking. Story drift values were then checked to evaluate if they satisfy ASCE 7-16 allowable story drift limits, and the strength and reinforcement detailing provided for beams, columns, joints, and walls were assessed to see if they satisfy ACI 318-19 requirements for special moment frames and special shear walls.

1.2 Organization

This report is organized into seven chapters. Chapter 2 provides a description of the test buildings, including member sizes and details, and also describes the test procedures. The 3D modeling approach used for the two buildings is described in Chapter 3 and results of the design assessments for the 2015 and 2018/2019 buildings (from now on they will be called as Building #1 and Building #2 respectively) are done in Chapters 4 and 5 respectively. Several sensitivity studies are presented in Chapter 6 to assess the influence of key modeling assumptions on the design assessment. Conclusions are presented in Chapter 7.

CHAPTER 2. TEST STRUCTURES AND EXPERIMENTAL RESULTS

E-Defense shaking table (Figure 2.1) has plan dimensions of 20 m by 15 m with a total load carrying capacity of 12000 kN [7]. The table can produce maximum velocities of 2.0 m/s in both orthogonal directions (x and y) and 0.7 m/s in the vertical direction (z). Also, the table displacement capacities are ±1.0 m and ±0.5 m in x-y and z directions, respectively. The structure tested in 2015 (Building #1) had first floor plan dimensions of 9.7 m in the transverse direction (x dir.) and 15.7 m in the longitudinal direction (y dir.). For the upper stories, these dimensions were decreased to 9.5 m and 13.5 m, respectively. The floor heights were 2.80 m for the first floor, 2.6 m from 2^{nd} to 4^{th} floor, 2.55 m for the 5^{th} to 7^{th} floors and 2.5 m for the top 3 floors. Figure 2.2 shows the plan and elevation views of the 2015 test structure.

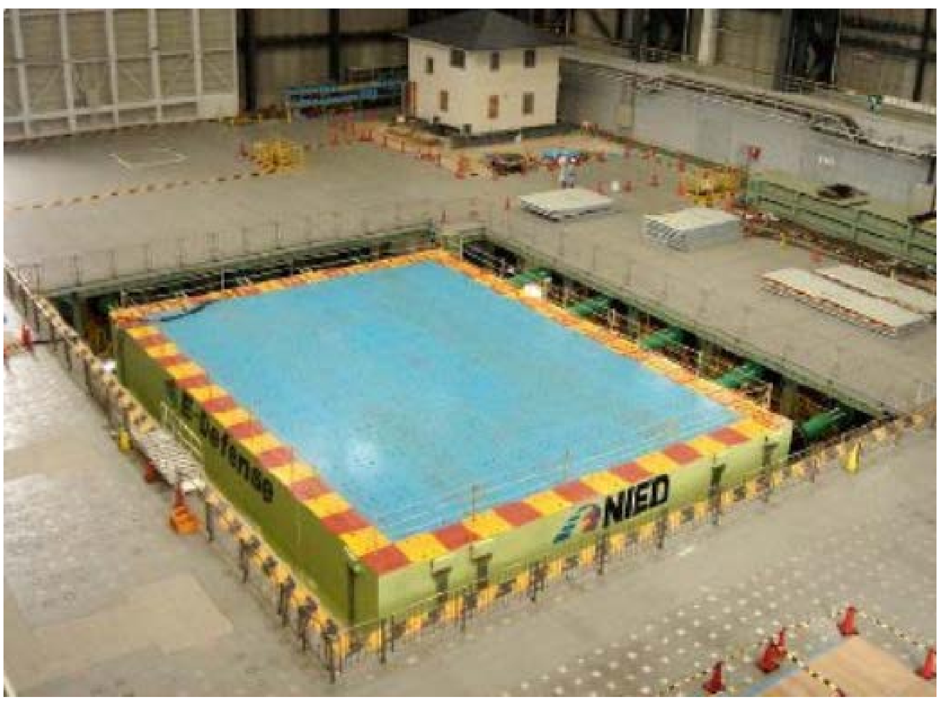

Figure 2.1 E-Defense Shaking Table [7]

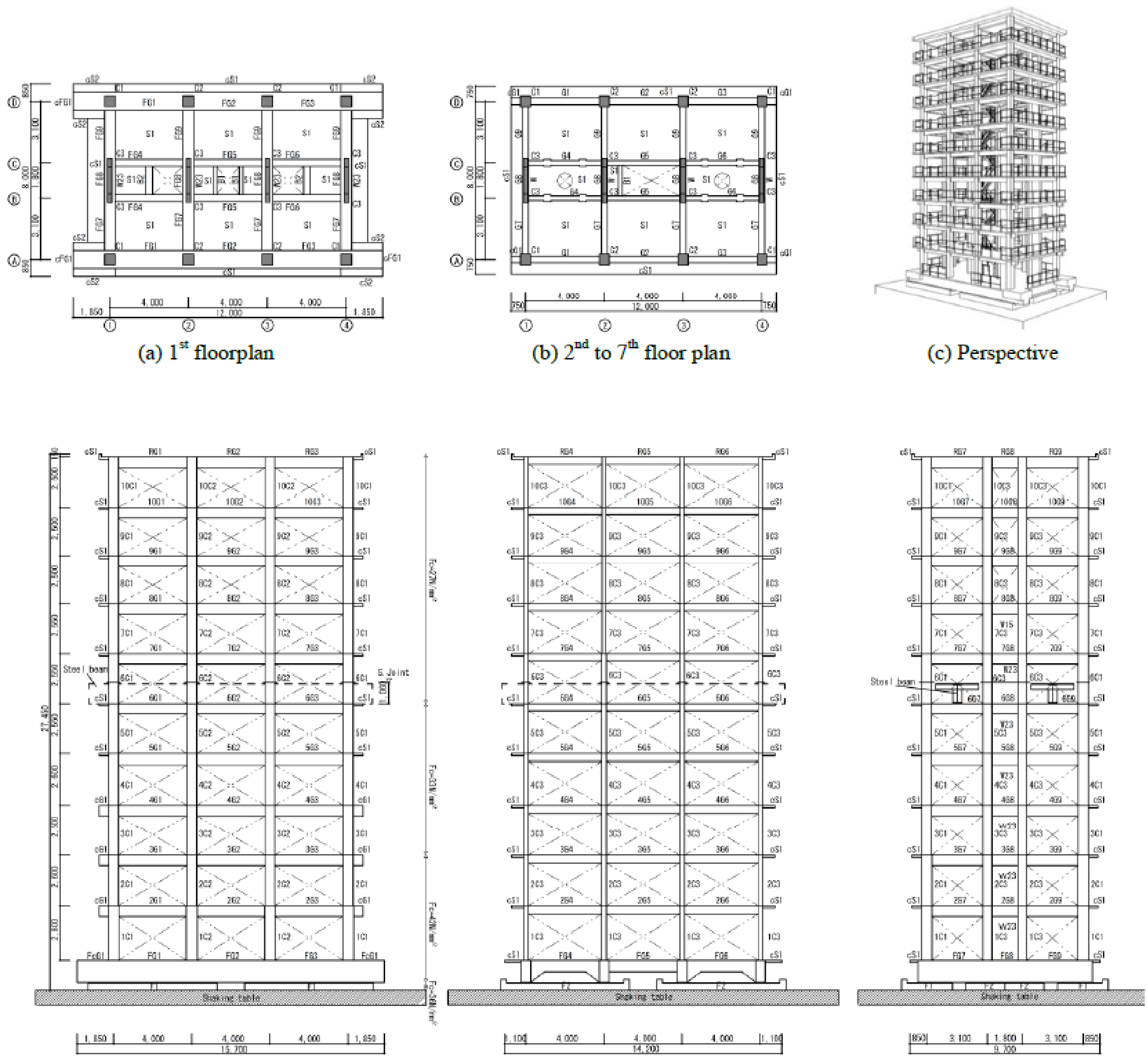

(a) 1st floorplan (b) 2nd to 7th floor plan (c) Perspective

(d) A, D frame (e) B, C frame (f) 1-4 Frame

Figure 2.2 Plan and elevation views of 2015 test structure [4]

The lateral-force-resisting systems for the test building consisted of special reinforced concrete moment frames in the longitudinal (y) direction and special reinforced concrete shear walls in the transverse (x) direction. The three-bay perimeter moment frame had centerline bay widths of 4 m. Perimeter columns (C1 and C2 columns) were 550 mm by 550 mm for the first story, 500 mm by 550 mm for the second story and 500 mm x 550 mm for the remaining stories (3-10). The beams (G1, G2 and G3) framing between perimeter columns were 550 mm deep and 350 mm wide for floors 2 through 7, and 500 mm deep and 300 mm wide at floors 8, 9 and 10, and at the roof level. The four structural (shear) walls comprising the lateral system in the x-direction were

2.25 m long with 230 mm thick webs from the base to the 7th floor, and 150 mm thick webs above the 7th floor. The wall webs were terminated at the 8th floor such that the boundary columns, along with beams spanning to the building perimeter columns provided the lateral resistance at the upper three levels. Provided longitudinal and transverse reinforcement for the end sections (boundary columns) of the walls were identical to C3 columns. Two curtains of web vertical reinforcement, 13 mm diameter bars spaced at 250 mm on center were provided over the first story (W23A) and for the 2nd through 7th stories (W23), whereas spacing of web transverse reinforcement was 150 mm on center. Above this level, for the W15 walls, center-to-center distance of the 10 mm bars for the two curtains of web vertical and transverse reinforcement were 200 mm. Table 2.1 summarizes the cross-sectional dimensions of the perimeter columns and beams, walls, and the slabs.

Table 2.1 Member Section Sizes, Building #1

2015												
Floor	Height (mm)	Columns				Beams				Wall	Slab	
		C1		C2		G1-G3		G2		W1	S1	*f'c*
		B (mm)	D (mm)	B (mm)	D (mm)	B (mm)	D (mm)	B (mm)	D (mm)	t (mm)	t (mm)	Mpa
R						300	500	230	370		130	
10	2500	500	500	230	450	300	500	230	370	-	130	27
9	2500	500	500	230	450	300	500	230	370	-	130	27
8	2500	500	500	230	450	300	500	230	370	-	130	27
7	2550	500	500	230	450	350	550	230	370	150	130	27
6	2550	500	500	230	450	350	550	230	370	230	130	27
5	2550	500	500	230	450	350	550	230	370	230	130	33
4	2600	500	500	230	450	350	550	230	420	230	130	33
3	2600	500	500	230	450	350	550	230	420	230	130	33
2	2600	500	550	230	450	350	550	230	420	230	130	42
1	2800	550	550	230	450	900	1150	350	600	230	130	42

Figures 2.3 and 2.4 illustrate the design details of the columns and perimeter beams including the cross-sectional dimensions, number and the diameter of the longitudinal and transverse reinforcement. The details of the transverse reinforcement used in the beam-column joints are also shown in Figure 2.3.

		C1	C2	C3
10F	Joint	2, 2-D10@150	2, 2-D10@150	2, 2-D10@150
	B×D	500 × 500	500 × 500	230 × 450
	Section			
	Rebar	8 - HD19	10 - HD19	6 - LD16
	Hoop	LD10[2, 2]@100	LD10[2, 2]@100	LD10[2, 2]@100
9F	Joint	2, 2-D10@150	2, 2-D10@150	2, 2-D10@150
	B×D	500 × 500	500 × 500	230 × 450
	Section			
	Rebar	8 - HD19	10 - HD19	6 - LD16
	Hoop	LD10[2, 2]@100	LD10[2, 2]@100	LD10[2, 2]@100
8F	Joint	2, 2-D10@150	2, 2-D10@150	2, 2-D10@150
	B×D	500 × 500	500 × 500	230 × 450
	Section			
	Rebar	8 - HD19	10 - HD19	6 - HD19
	Hoop	LD10[2, 2]@100	LD10[3, 2]@100	LD10[2, 2]@100
7F	Joint	2, 2-D10@150	2, 2-D10@150	2, 2-D10@150
	B×D	500 × 500	500 × 500	230 × 450
	Section			
	Rebar	10 - HD22	10 - HD22	6 - HD19
	Hoop	LD10[2, 2]@100	LD10[3, 2]@100	LD10[2, 2]@100
6F	Joint	2, 2-D10@150	2, 2-D10@150	2, 2-D10@150
	B×D	500 × 500	500 × 500	230 × 450
	Section			
	Rebar	10 - HD22	12 - HD22	6 - HD19
	Hoop	LD10[2, 2]@100	LD10[4, 2]@100	LD10[2, 2]@100
5F	Joint	2, 2-D10@150	2, 2-D10@150	2, 2-D10@150
	B×D	500 × 500	500 × 500	230 × 450
	Section			
	Rebar	10 - HD22	12 - HD22	6 - HD19
	Hoop	LD10[2, 2]@100	S10[4, 2]@100	LD10[2, 2]@100
4F	Joint	2, 2-D10@150	2, 2-D10@150	2, 2-D10@150
	B×D	500 × 500	500 × 500	230 × 450
	Section			
	Rebar	10 - HD22	12 - HD22	6 - HD19
	Hoop	S10[2, 2]@100	S10[4, 2]@100	LD10[2, 2]@100
3F	Joint	2, 2-D10@150	2, 2-D10@150	2, 2-D10@150
	B×D	500 × 500	500 × 500	230 × 450
	Section			
	Rebar	12 - HD22	12 - HD22	6 - HD19
	Hoop	S10[2, 2]@100	S10[4, 2]@100	LD10[2, 2]@100
2F	Joint	2, 2-D10@150	2, 2-D10@150	2, 2-D10@150
	B×D	500 × 550	500 × 550	230 × 450
	Section			
	Rebar	16 - HD22	12 - HD22	8 - HD19
	Hoop	S10[2, 2]@100	S10[4, 2]@100	LD10[2, 2]@100
1F	Joint	2, 2-D10@150	2, 2-D10@150	2, 2-D10@150
	B×D	550 × 550	550 × 550	230 × 450
	Section			
	Rebar	20 - HD22	16 - HD22	8 - HD19
	Hoop	S10[4, 4]@100	S10[4, 4]@100	S10[4, 2]@100

Figure 2.3 Reinforcement Details of Columns, Building #1 [4]

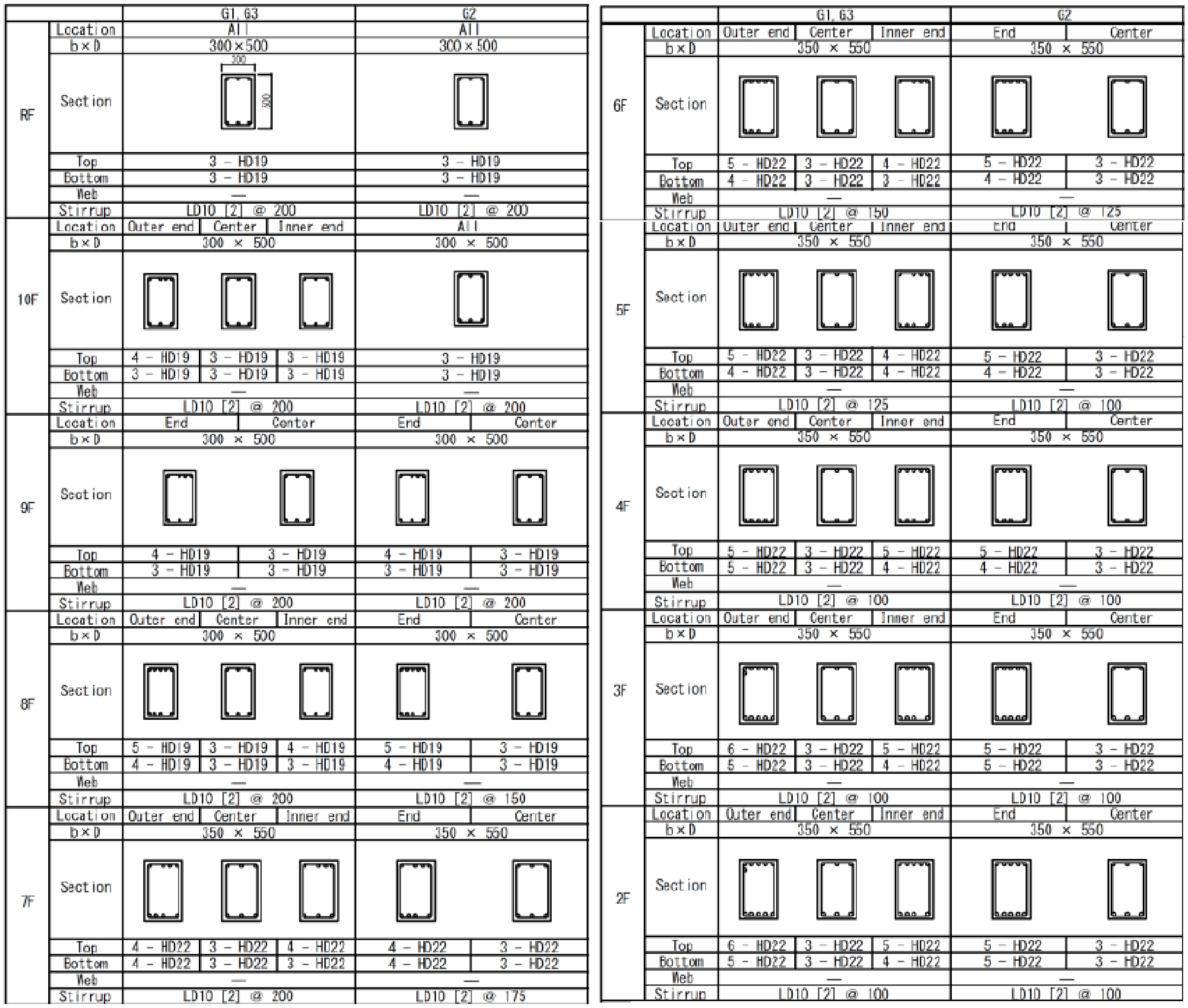

Figure 2.4 Reinforcement Details of Perimeter Beams, Building #1 [4]

Although during the experiments concrete and reinforcing rebars were tested and reported at every floor, the design material strengths were used for the assessment of the buildings in this work. Table 2.2 summarizes the design concrete and rebar strengths.

Table 2.2 Design Material Properties, Building #1

Concrete		**Reinforcing bars**				
	f'c (MPa)		Grade	A_{normal} (mm^2)	σ_y (MPa)	σ_t (MPa)
Floors 1 and 2	42	D22	SD345	387	345	490
Floors 3,4 and 5	33	D19	SD345	287	345	490
Floors 6 - Roof	27	D13	SD295A	127	295	440
		D10	SD295A	71	295	440
		S10	KSS785	71	785	930

During the testing, recorded ground motions of JMA Kobe earthquake were applied with increasing intensities (10%, 25%, 50% and 100%) in all of the three principal directions (x, y and vertical). Figure 2.5 shows time history series and the response history of the ground motions of the JMA Kobe scaled 100% where NS represents the frame direction (y dir.), EW represents the wall direction (x dir.), and UD is the vertical ground motion.

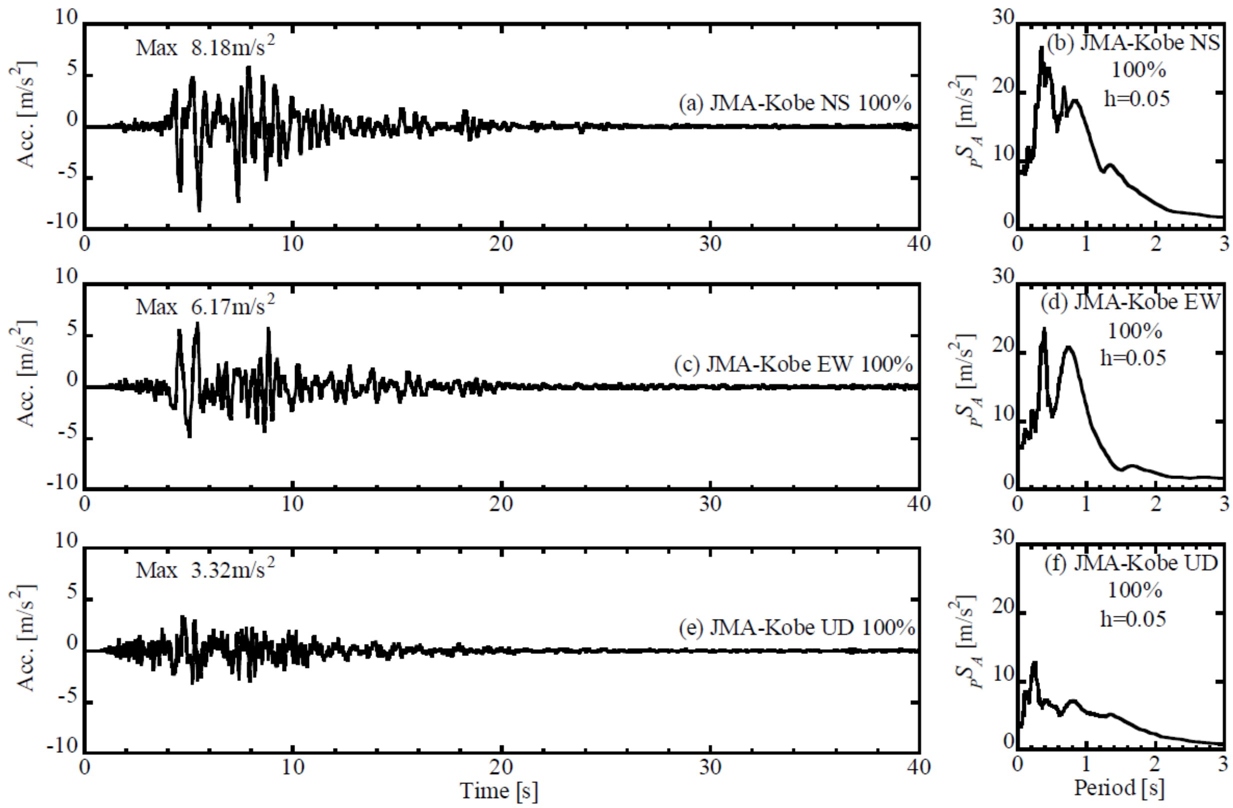

Figure 2.5 Wave time histories and the response spectrums [11]

Experiments were performed in two stages; in stage 1, the foundations of the buildings were not fixed at the shaking table. Therefore, structures were allowed to slip on top of some cast iron bearings (Base slip stage). After the shaking of the structures with slipping base and increasing excitations, foundations were fixed to the shaking table (Fixed base stage) and ground motions were applied one more time. Table 2.3 shows the natural periods and the maximum story drift angles for Building #1 after each excitation for both the frame and wall directions.

Table 2.3 Natural Periods and the Maximum story drift angles, 2015 [11]

No.	Input wave		Test case	Natural Period [s]		Maximum story drift angle [rad]	
				Frame direction	Wall direction	Frame direction	Wall direction
-	Initial		Base slip	0.57	0.57	-	-
1	JMA-Kobe	10%		0.61	0.61	0.0011	0.0006
2		25%		0.69	0.63	0.0026	0.0010
3		50%		0.76	0.64	0.0041	0.0017
4		100%		0.87	0.69	0.0060	0.0030
-	Initial		Fixed base	0.85	0.58	-	-
5	JMA-Kobe	10%		0.87	0.58	0.0028	0.0008
6		25%		0.94	0.60	0.0075	0.0022
7		50%		1.24	0.74	0.0171	0.0065
8		100%		2.43	1.13	0.0305	0.0150
9		60%		2.62	1.19	0.0131	0.0122

In terms of the damage, under the 100% excitation and for the fixed base stage, beam-column joint shear failures were observed at the 3rd, 4th and 5th floors for the 2015 test structure. Also, concrete cover spalling at the base of 1st floor corner columns and minor concrete crushing at the base shear wall were observed (Figure 2.6). More information on the test procedure, specimen design, instrumentation and experimental results of the 2015 tests can be found on Kajiwara et al. [4], Sato et al. [9] and Tosauchi et al. [11].

(a) 4th story beam-column joint (b) 1st floor column base (c) 1st floor wall base

Figure 2.6 Specimen Damage, 2015 tests [11]

For Building #2, the overall geometry of the building was essentially unchanged, except that the width of the cantilever slab around the building perimeter was decreased to 700 mm from 750 mm. Based on the damage observed in Building #1, the cross-sectional dimensions of some of the members were modified. The modifications done on the dimensions of the perimeter column and beams, and also of the walls and slabs are summarized in Table 2.4 (where cells highlighted in yellow indicate changes). The last column of Table 2.4 shows the design strength of the concrete used at every floor. The comparison with Table 2.1 shows that the design concrete strengths are the same for both buildings, except for the first two floors.

Table 2.4 Member Dimension of the Building #2

2018												
Floor	Height (mm)	Columns				Beam				Wall	Slab	
		C1		C2		G1-G3		G2		W1	S1	*f'c*
		B (mm)	D (mm)	B (mm)	D (mm)	B (mm)	D (mm)	B (mm)	D (mm)	t (mm)	t (mm)	Mpa
R						250	450	230	370		100	27
10	2500	500	500	230	450	250	450	230	370	-	100	27
9	2500	500	500	230	450	300	450	230	370	-	100	27
8	2500	500	500	230	450	300	450	230	370	-	100	27
7	2550	500	500	230	450	300	500	230	370	120	100	27
6	2550	500	500	230	450	300	500	230	370	150	100	27
5	2550	500	500	230	450	320	500	230	370	150	100	33
4	2600	500	500	230	450	320	500	230	420	150	100	33
3	2600	500	500	230	450	320	500	230	420	150	100	33
2	2600	500	550	230	450	320	500	230	420	150	100	39
1	2800	550	550	230	450	900	1150	350	600	150	100	39

Along with the section dimensions, longitudinal and transverse reinforcements of the some of the members were also altered for the Building #2. The reinforcement design of the columns of the structure is given in Figures 2.7 and 2.8 from 1st to 5th floors and from 6th to 10th floors respectively. Details of the transverse reinforcement used at the beam-columns joint zones are also given in these figures in terms of the number of the stirrup legs (n), the vertical spacing (s) and the bar diameter.

Floor	Item		C1				C2				C3			
5F	Joint		n		s	diameter (LD)	n		s	diameter (LD)	n		s	diameter (LD)
			6	6	70	10	6	6	70	10	3	2	150	10
	b x d		500		500		500		500		230		450	
	Section		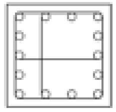				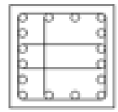				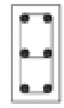			
	Rebar		n		diameter (HD)		n		diameter (HD)		n		diameter (HD)	
			14		22		16		22		6		19	
	Hoop		n		s	diameter (LD)	n		s	diameter (LD)	n		s	diameter (LD)
		Axis	3	3	100	10	4	3	100	10	3	2	100	10
		Head / Leg	6	6	70	10	6	6	70	10	3	2	100	10
4F	Joint		n		s	diameter (LD)	n		s	diameter (LD)	n		s	diameter (LD)
			6	6	70	10	6	6	70	10	3	2	150	10
	b x d		500		500		500		500		230		450	
	Section		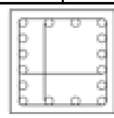				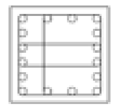				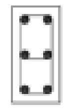			
	Rebar		n		diameter (HD)		n		diameter (HD)		n		diameter (HD)	
			16		22		16		22		6		19	
	Hoop		n		s	diameter (LD)	n		s	diameter (LD)	n		s	diameter (LD)
		Axis	3	3	100	10	4	3	100	10	3	2	100	10
		Head / Leg	6	6	70	10	6	6	70	10	3	2	100	10
3F	Joint		n		s	diameter (LD)	n		s	diameter (LD)	n		s	diameter (LD)
			6	6	70	10	6	6	70	10	3	2	150	10
	b x d		500		500		500		500		230		450	
	Section		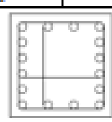				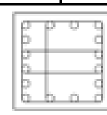				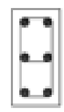			
	Rebar		n		diameter (HD)		n		diameter (HD)		n		diameter (HD)	
			16		22		16		22		6		19	
	Hoop		n		s	diameter (LD)	n		s	diameter (LD)	n		s	diameter (LD)
		Axis	3	3	100	10	4	3	100	10	3	2	100	10
		Head / Leg	6	6	70	10	6	6	70	10	3	2	100	10
2F	Joint		n		s	diameter (LD)	n		s	diameter (LD)	n		s	diameter (LD)
			6	6	60	10	6	6	60	10	3	2	150	10
	b x d		500		550		500		550		230		450	
	Section		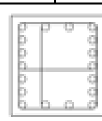				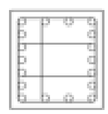				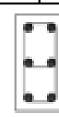			
	Rebar		n		diameter (HD)		n		diameter (HD)		n		diameter (HD)	
			18		22		18		22		6		19	
	Hoop		n		s	diameter (LD)	n		s	diameter (LD)	n		s	diameter (LD)
		Axis	3	3	100	10	4	3	100	10	3	2	100	10
		Head / Leg	6	6	60	10	6	6	60	10	3	2	100	10
1F	Joint		n		s	diameter (LD)	n		s	diameter (LD)	n		s	diameter (LD)
			6	6	60	10	6	6	60	10	3	2	150	10
	b x d		550		550		550		550		230		450	
	Section		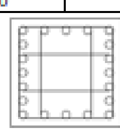				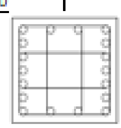				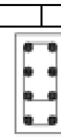			
	Rebar		n		diameter (HD)		n		diameter (HD)		n		diameter (HD)	
			20		22		18		22		8		19	
	Hoop		n		s	diameter (LD)	n		s	diameter (LD)	n		s	diameter (LD)
		Axis	4	4	100	10	4	4	100	10	3	2	100	10
		Head / Leg	6	6	60	10	6	6	60	10	3	2	100	10

Figure 2.7 First floor to 5th floor column reinforcement details, Building #2

			C1				C2				C3			
10F	Joint		n		s	diameter (LD)	n		s	diameter (LD)	n		s	diameter (LD)
			6	6	85	10	6	6	85	10	3	2	150	10
	b x d		500		500		500		500		230		450	
	Section		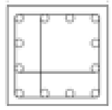				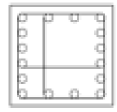				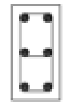			
	Rebar		n		diameter (HD)		n		diameter (HD)		n		diameter (HD)	
			12		22		16		22		6		19	
	Hoop		n		s	diameter (LD)	n		s	diameter (LD)	n		s	diameter (LD)
		Axis	3	3	100	10	3	3	100	10	3	2	100	10
		Head / Leg	6	6	85	10	6	6	85	10	3	2	100	10
9F	Joint		n		s	diameter (LD)	n		s	diameter (LD)	n		s	diameter (LD)
			6	6	85	10	6	6	85	10	3	2	150	10
	b x d		500		500		500		500		230		450	
	Section		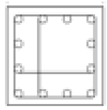				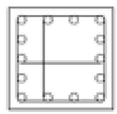				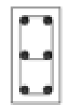			
	Rebar		n		diameter (HD)		n		diameter (HD)		n		diameter (HD)	
			12		22		14		22		6		19	
	Hoop		n		s	diameter (LD)	n		s	diameter (LD)	n		s	diameter (LD)
		Axis	3	3	100	10	3	3	100	10	3	2	100	10
		Head / Leg	6	6	85	10	6	6	85	10	3	2	100	10
8F	Joint		n		s	diameter (LD)	n		s	diameter (LD)	n		s	diameter (LD)
			6	6	85	10	6	6	85	10	3	2	150	10
	b x d		500		500		500		500		230		450	
	Section		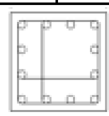				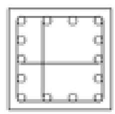				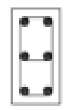			
	Rebar		n		diameter (HD)		n		diameter (HD)		n		diameter (HD)	
			12		22		14		22		6		19	
	Hoop		n		s	diameter (LD)	n		s	diameter (LD)	n		s	diameter (LD)
		Axis	3	3	100	10	3	3	100	10	3	2	100	10
		Head / Leg	6	6	85	10	6	6	85	10	3	2	100	10
7F	Joint		n		s	diameter (LD)	n		s	diameter (LD)	n		s	diameter (LD)
			6	6	85	10	6	6	85	10	3	2	150	10
	b x d		500		500		500		500		230		450	
	Section		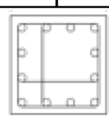				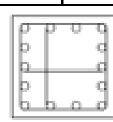				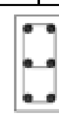			
	Rebar		n		diameter (HD)		n		diameter (HD)		n		diameter (HD)	
			12		22		14		22		6		19	
	Hoop		n		s	diameter (LD)	n		s	diameter (LD)	n		s	diameter (LD)
		Axis	3	3	100	10	3	3	100	10	3	2	100	10
		Head / Leg	6	6	85	10	6	6	85	10	3	2	100	10
6F	Joint		n		s	diameter (LD)	n		s	diameter (LD)	n		s	diameter (LD)
			6	6	85	10	6	6	85	10	3	2	150	10
	b x d		500		500		500		500		230		450	
	Section		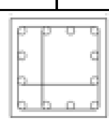				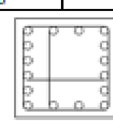				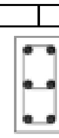			
	Rebar		n		diameter (HD)		n		diameter (HD)		n		diameter (HD)	
			12		22		16		22		6		19	
	Hoop		n		s	diameter (LD)	n		s	diameter (LD)	n		s	diameter (LD)
		Axis	3	3	100	10	3	3	100	10	3	2	100	10
		Head / Leg	6	6	85	10	6	6	85	10	3	2	100	10

Figure 2.8 6th floor to 10th floor column reinforcement details, Building #2

The main changes on the reinforcement detailing of Building #2 columns were made on the transverse reinforcement due to the shear failures observed on the beam-column joints and the columns' end zones near the joints. While for the Building #1 the shear reinforcement spacing and the amount of the shear reinforcement was kept constant throughout the height of column in one story, for Building #2, columns were divided into 3 zones in terms of the shear reinforcement detailing; head, axis and the leg (see Figures 2.7 and 2.8). The head and leg portions of the columns represent a zone from joint face to a height equals to the columns depth where these zones were heavily reinforced, Figure 2.9.

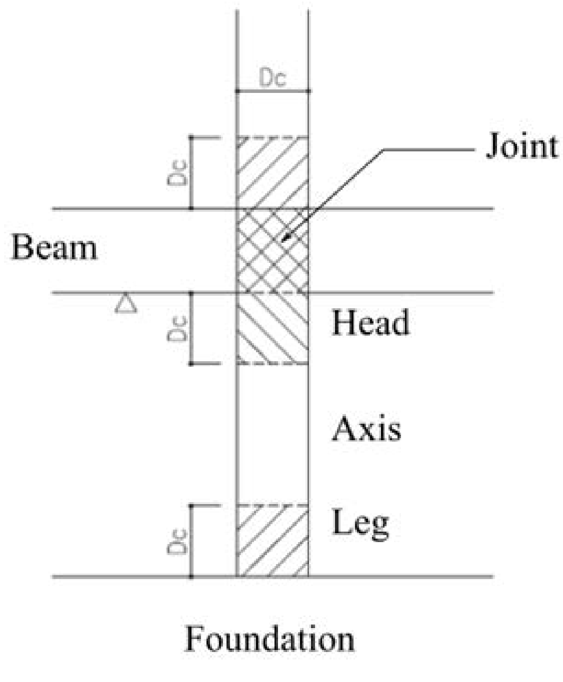

Figure 2.9 An illustration of Building #2 columns

Along with the columns, joints' shear reinforcement was increased too. Not only the spacing of the reinforcement was decreased from 150 mm to 60 mm for the first two floors, to 70 mm for the 3rd, 4th and 5th floors, and to 85 mm for the upper floors but also the amount of rebar used was increased from two bars in each orthogonal direction to six bars.

CHAPTER 3. 3D ELASTIC MODELS

As mentioned before, the main purpose of this report is to assess the designs of 2015 and 2018 test structures using American standards. To this end, a relatively simple analysis type which is the linear elastic analysis is chosen. 3D models of the structures are created using a structural engineering software called ETABS based on the information given in Chapter 2. Two different models were created (one for the frame dir. and one for the wall dir.) for both of the structures. The reason behind creating different models for different directions is that the boundaries of the walls were designed as columns. Therefore, while for the wall direction model (from now on will be called as Wall model), only shell elements were used for the entire wall, for the frame dir. model (from now on will be called as Frame model), a column (line element) – wall web (shell element) – column (line element) member is used for the walls, see Figures 3.1 and 3.2. For the Frame model, line elements (boundary columns) and the shell elements were connected with rigid frames so that they can deform similarly. A sensitivity study which shows the behavior of these two different models is given in Chapter 6.

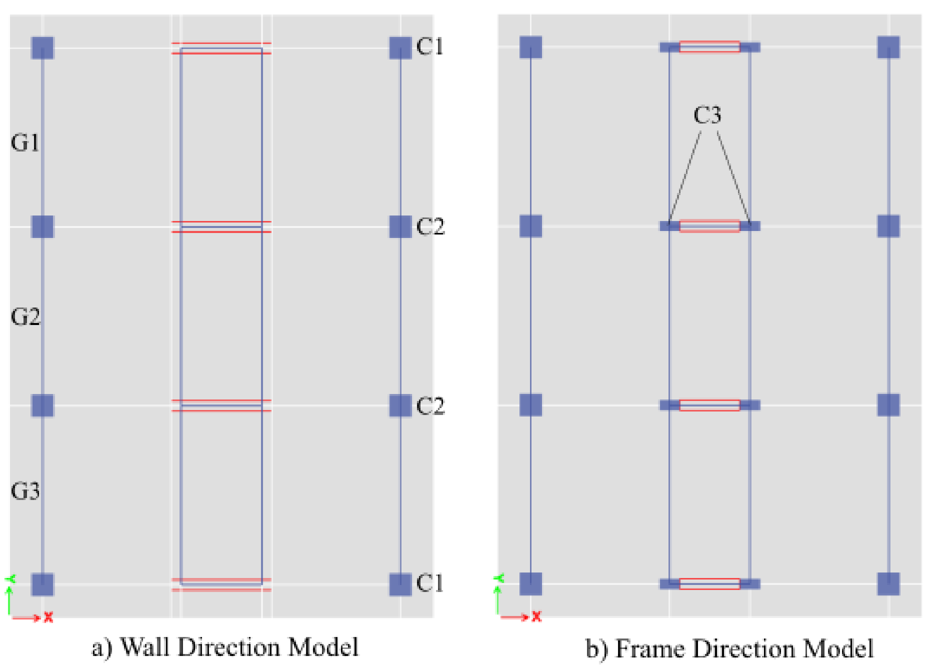

Figure 3.1 Plan View of the Models

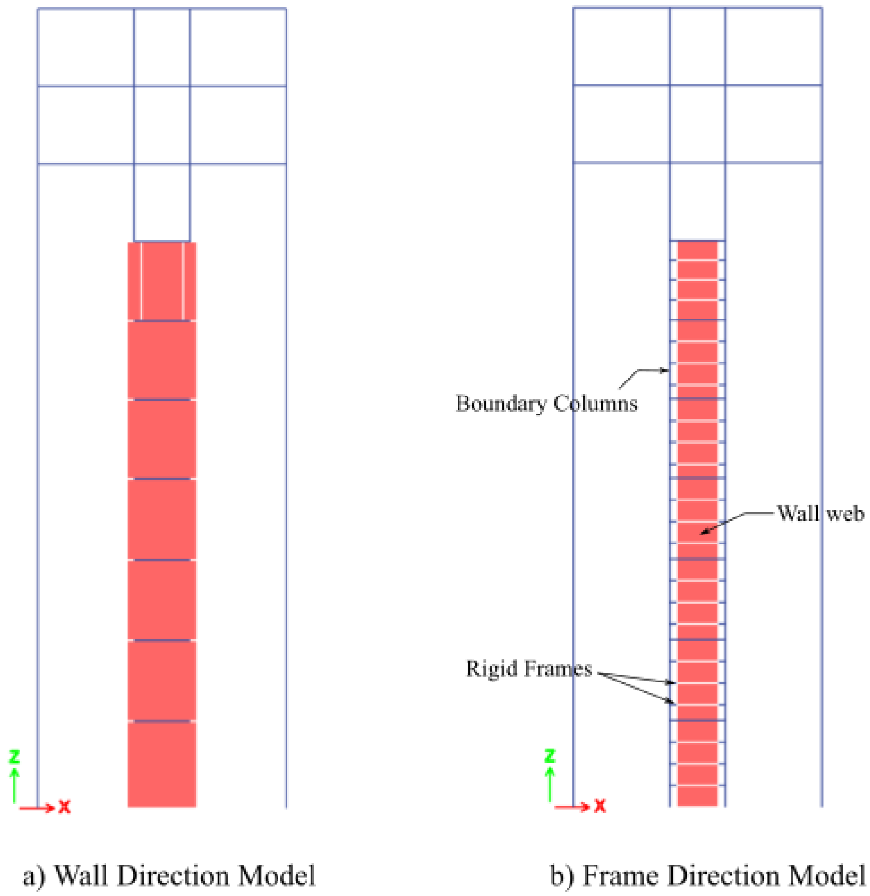

Figure 3.2 Elevation View of the Models

According to ASCE 7-16 §12.2.5.1, for a lateral load carrying system to be identified as a dual system, moment frames shall be capable of resisting at least 25% of the design seismic forces. Analysis results showed that this requirement is not satisfied with the test structures. Therefore, the seismic force resisting system in the wall direction is identified as special reinforced concrete walls (Cd=5, R=5). To this end, G7 and G9 beams (Figure 2.2), beams that connect the walls to the perimeter columns, are not included in the models, and therefore the models consist of only the structural walls in the wall direction. In Chapter 6, analysis results of a model which contains the G7 and G9 beams are shown to be able to understand the effects of not including these beams in the models.

Based on the response spectrums given in Figure 2.5, it is found that spectral response acceleration parameter at a period of 1 second (S_1) is 1.2 seconds in the wall direction and 1.5 seconds in the frame direction. Therefore, according to ASCE 7-16 §11.6, Seismic Design Categories of the structures are Category E. It is stated in §12.5 that, if the structures in Seismic Design Category E do not have Type 5 horizontal structural irregularity, then the seismic forces can be applied independently in each of two orthogonal directions, and orthogonal interaction effects are permitted to be neglected. Since the structures in question do not possess Type 5 irregularity, the loadings are applied independently. Also, according to §12.9.1.4, where the modal base shear (V_t) is less than the calculated base shear (V) using equivalent lateral force procedure, the forces shall be multiplied by V/V_t. Additionally, if V_t is less than C_s*W, where C_s is determined in accordance with Eq. 12.8-6 and W is the effective seismic weight of the structure, drifts shall be multiplied by C_s*W/V_t. However, in this study, since the purpose is to assess the buildings under the experimental loading conditions, apart from R/I_e factor where R is the response modification coefficient (R=5 in the wall direction and R=8 in the frame direction) and I_e is the importance factor (I_e=1), no force or drift scaling is done. To be consistent, no load factors were applied to the gravity loads and therefore the load combinations used as follows,

$$D + E_V + E_h \tag{3.1}$$

$$D - E_V + E_h \tag{3.2}$$

where D is the dead load (mass calculations are given in the following pages), E_v is the vertical seismic load effects (taken as $0.2S_{DS}D$) and E_h is the horizontal seismic load effect. E_h is calculated as:

$$E_h = \rho Q_E \tag{3.3}$$

where ρ is the redundancy factor and Q_E is the effects of horizontal seismic forces from V (total design lateral force). The redundancy factor is calculated in accordance with §12.3.4.2 where it is stated that ρ should be taken as 1.3 for the structures under the Seismic Design Category E unless each story resists more than 35% of the base shear or each story that resists more than 35% of the base shear consist of at least two bays of seismic force-resisting perimeter framing on each side of the structure. It is found that, for both Building #1 and Building #2, roof level and the 10^{th} floor do not carry at least 35% of the base shear, and the stories that carry this load do not have 2 bays of perimeter framing. The number of the bays for the shear walls are calculated as the length of shear wall divided by the story height, e.g., for the first-floor number of the bays are equal to 2250 mm/2800 mm = 0.8. Therefore, a redundancy factor of 1.3 is applied for the calculations of member forces. However, for the drifts, it is allowed to use a redundancy factor of one (§12.3.4.1).

Weights of the structures were aimed to match with the actual experimental values. Therefore, on top of the self-weight of the members obtained from ETABS, distributed dead loads are applied at each floor until the weight of each is approximately same as the values reported. Details of the structures' weights are given in Table 3.1.

Table 3.1 Floor masses of the Structures

Building #1					Building #2				
Floor	Height (m)	Live L.(kN)	Dead L. (kN)	Sum (kN)	Floor	Height (m)	Live L.(kN)	Dead L. (kN)	Sum (kN)
R	-	0.0	725.0	725.0	R	-	0.0	579.0	579.0
10	2.5	57.0	740.0	1522.0	10	2.5	57.0	706.0	1342.0
9	2.5	28.0	694.0	2244.0	9	2.5	28.0	639.0	2009.0
8	2.5	28.0	716.0	2988.0	8	2.5	28.0	657.0	2694.0
7	2.6	28.0	949.0	3965.0	7	2.6	29.0	721.0	3444.0
6	2.6	188.0	618.0	4771.0	6	2.6	188.0	870.0	4502.0
5	2.6	28.0	780.0	5579.0	5	2.6	28.0	716.0	5246.0
4	2.6	28.0	798.0	6404.0	4	2.6	28.0	732.0	6006.0
3	2.6	28.0	817.0	7250.0	3	2.6	28.0	750.0	6784.0
2	2.6	57.0	889.0	8196.0	2	2.6	57.0	848.0	7689.0
1	2.8	29.0	1830.0	10055.0	1	2.8	29.0	1827.0	9545.0

Also, instead of modeling the beams of the structures as rectangular beams with the dimensions given in Tables 2.1 and 2.4, T sections are used where the effective overhanging flange widths are calculated based on the requirements given in ACI 318. Different models were created with rectangular beams and slabs as shell elements with the given thickness and the appropriate stiffness modifiers and compared with the models where only T-Beams are used. The comparisons were mainly focused on the buildings' periods, to see the effects of different modeling approaches on the stiffness of the buildings since the story masses are matched with the experimental values, and similar results were obtained. The reason behind choosing the T-Beam model is because rectangular beams and slabs (shell elements) are used for the modeling approach, and the forces taken by the slab have to be considered during the design check. Depending on the relative stiffnesses of the slab and beam sections, shell elements might carry substantial forces. Various modeling approaches for the slabs and the beams are studied, including the option to use a rigid in-plane floor diaphragm. It is observed that assigning rigid diaphragms to the floors influenced the periods of the buildings greatly, around 20-25% decreases are observed in first mode periods in the frame directions. Based on the provisions of ASCE 7, rigid diaphragms are assigned at each floor.

Finally, the moment of inertias of the members are calculated by using the stiffness multipliers which are based on ACI 318-19 Table 6.6.3.1.1(a). They are taken as 0.7 for columns, 0.35 for the walls and the beams, and 0.25 for slabs, refer to Table 3.2.

Table 3.2 Moment of Inertias and Cross-Sectional Areas [1]

<table>
<tr><th colspan="2">Member and condition</th><th>Moment of inertia</th><th>Cross-sectional area for axial deformations</th><th>Cross-sectional area for shear deformations</th></tr>
<tr><td colspan="2">Columns</td><td>$0.70I_g$</td><td rowspan="5">$1.0A_g$</td><td rowspan="5">b_wh</td></tr>
<tr><td rowspan="2">Walls</td><td>Uncracked</td><td>$0.70I_g$</td></tr>
<tr><td>Cracked</td><td>$0.35I_g$</td></tr>
<tr><td colspan="2">Beams</td><td>$0.35I_g$</td></tr>
<tr><td colspan="2">Flat plates and flat slabs</td><td>$0.25I_g$</td></tr>
</table>

CHAPTER 4. ASSESSMENT OF 2015 TEST STRUCTURE

This chapter focuses on the assessment of 2015 test structure (Building #1) using ACI 318-19 [1] provisions where the plan and elevation views, and the member details of the structure are given in Figures 2.2, 2.3 and 2.4 respectively. The model and the loading conditions used to calculate the demands are explained in Chapter 3.

4.1 Shear Walls

Lateral force resisting system of the structure in the x direction consists of 4 identical special reinforced concrete shear walls with a total length of 2250 mm and with a thickness of 230 mm (thickness of the wall web decreases to 150 mm after the 7th floor, W15 walls). Walls are constructed to be continuous from the base of the structure to the 8th floor (for the upper three stories, moment frames are used in both directions). Therefore, the total height of the walls are 18.25 meters (59.87*ft*). Figure 4.1 shows the cross-sections of the walls at the first floor (W23A), 2nd through 6th floors (W23) and at the 7th floor (W15).

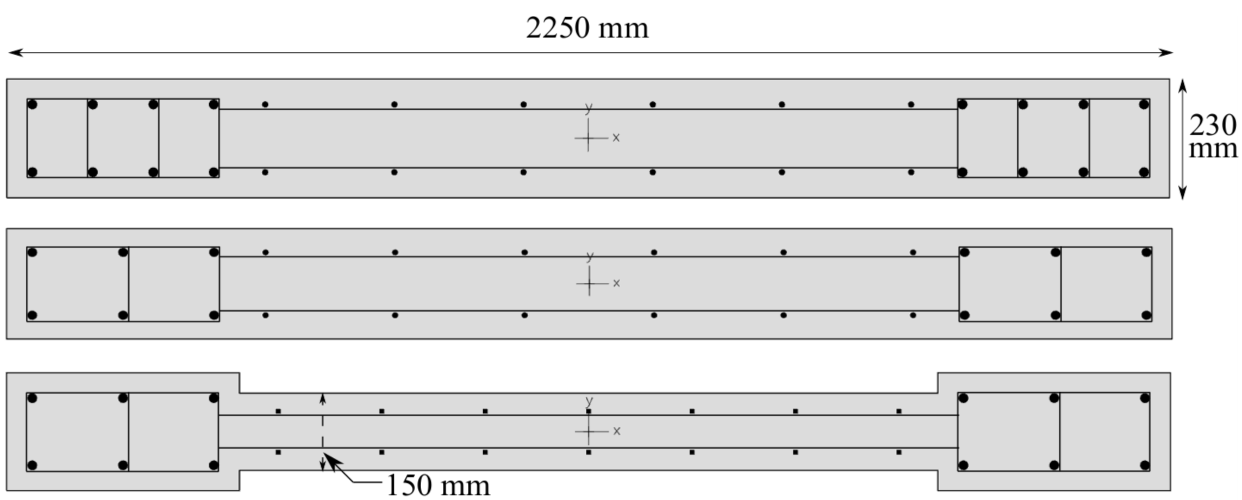

Figure 4.1 W23A and second floor W23 (top), W23 (middle) and W15 (bottom) walls

Combined axial force-moment strength of the walls are calculated using the P-M interaction diagrams. Demands at the base and at the top of first story walls are shown in Figure 4.2 where they are compared with the ϕP-ϕM capacity. The strength reduction factors (ϕ) are calculated based on ACI 318-19 §21.2. It is found that at base of the perimeter walls, a base moment of M_u

= 1466 k-ft is produced with a maximum axial load of P_u = 190 kips (845.2 kN) for the load combination 1 (Eqn. 3.1). For the load combination 2 (Eqn. 3.2) axial forces are decreased to the minimum value of P_u = 130 kips. Therefore, it is concluded that the axial load demands on the W23A perimeter walls are much lower than the total axial load capacity, $P_u/A_g f'_c$ = 845.2 kN / (0.23 m * 2.25 m) * (42MPa) = 0.039. This ratio is a little bit higher for inner walls, $P_u/A_g f'_c$ = 1135 kN / (0.23 m * 2.25 m) * (42MPa) = 0.052. Although Figure 4.2 shows the capacity versus demand comparison only for the W23A walls, similar comparisons are also made for the walls at the upper stories, and it is concluded that all the structural walls in Building #1 satisfy the P-M strength.

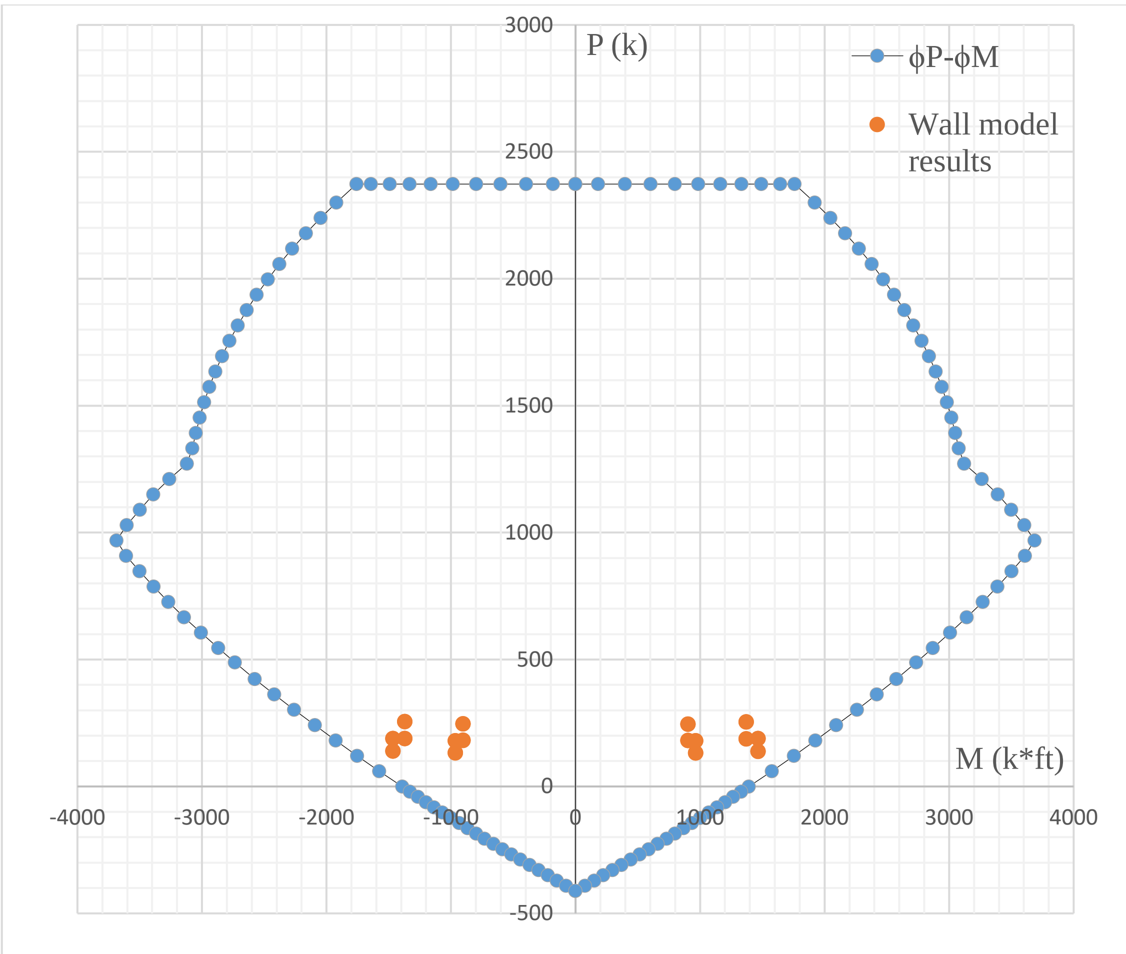

Figure 4.2 ϕP-ϕM interaction diagram of W23A walls

Shear strength of the structural walls (V_n) are calculated in accordance with ACI 318-19 §18.10.4,

$$V_n = \left(\alpha_c \lambda \sqrt{f_c'} + \rho_t f_{yt}\right) A_{cv} \tag{4.1}$$

where α_c= 3 for $h_w/l_w \leq 1.5$ and α_c= 2 for $h_w/l_w \geq 2.0$, and λ is taken as 1 for the normal-weight concrete. Since h_w/l_w = 59.87 ft / 7.38 ft = 8.11, α_c is taken as two. It should be noted here that V_n cannot be taken greater than $8\sqrt{f_c'}A_{cv}$ (§18.10.4.4). The design shear force V_e is calculated by the following formula:

$$V_e = \Omega_v \omega_v V_u \leq 3V_u \tag{4.2}$$

where V_u is the shear force obtained from lateral load analysis. Overstrength factor Ω_v is taken in accordance with Table 18.10.3.1.2 and ω_v is calculated based on the following equation.

$$\omega_v = 1.3 + \frac{n_s}{30} \leq 1.8 \tag{4.3}$$

where n_s is the number of stories above the critical section. Based on the Equations 4.1, 4.2 and 4.3 shear strength capacity and the design shear forces are calculated and given in Table 4.1. Since the 3rd, 4th and 5th floor walls have the same section detailing and the same material properties, they have the same factored shear strength and highest design shear forces is shown in the table. It can be observed from the table that $V_e/\phi V_n$ ratio is lower than the unity for the walls at every floor. Therefore, the shear reinforcement design of the shear walls satisfies the ACI 318-19 provisions.

Table 4.1 Shear strength and the design shear forces of the shear walls

	ϕV_n (kips)	V_e (kips)	$V_e/\phi V_n$
F1	251.53	163.39	0.65
F2	211.10	146.39	0.69
F3-4-5	200.43	146.75	0.73
F6	192.49	106.67	0.55
F7	137.00	113.51	0.83

ACI 318-19's minimum distributed web reinforcement ratios, ρ_l and ρ_t, are defined as 0.0025 (§18.10.2.1). Calculations showed that these minimum ratios are satisfied at every floor. $\rho_{l,min}$ within $0.15l_w$ from the end of a vertical wall segment is also set with the ratio of $6\sqrt{f_c'}/f_y$ (§ 18.10.2.4a). The minimum required amount and the used values are compared in Table 4.2.

Table 4.2 Comparison of ρ_l within 0.15lw

18.10.2.4a	$0.15\ l_w$ (mm)	337.5	
	$6\sqrt{f_c'}/f_y$	# bars in $0.15\ l_w$	ρ_l
F1-2	0.0093	6	0.021
F3-4-5	0.0082	4	0.014
F6-7	0.0075	4	0.014

Also, at least two curtains of reinforcement shall be used in the wall if $V_u > 2\lambda\sqrt{f_c'}A_{cv}$ (§18.10.2.2). Table 4.3 shows the comparison between the required and used number of vertical reinforcement curtains.

Table 4.3 Required and used number of reinforcement curtains

Number of Curtains	Required	Used
F1	2	2
F2	2	2
F3-4-5	2	2
F6	2	2
F7	2	2

Boundaries of the walls must be checked in accordance with §18.10.6. According to §18.10.6.2, whether special boundary elements (SBE) should be used or not depends on the following comparison,

$$\frac{1.5\delta_u}{h_{wcs}} \geq \frac{l_w}{600c} \tag{4.4}$$

where δ_u is calculated by multiplying the elastic displacements which is obtained from the elastic analysis on top of the 7th floor walls with C_d/I_e ratio (5/1). c corresponds to the largest neutral axis depth calculated for the factored axial force and nominal moment strength. Table 4.4 shows the calculated values for these ratios for the corner and inner walls. Since the requirement given in Equation 4.4 is satisfied, transverse reinforcement of the wall boundaries must satisfy the SBE provisions.

Table 4.4 SBE Requirement Check

	$1.5*\delta_u/h_{wcs}$	$l_w/600c$
Inner Walls	0.022	0.011
Corner Walls	0.023	0.012

After it is found that SBEs are required, the second step is to find how far the transverse reinforcement of SBSs are going to extend vertically above and below the critical section. To this end, two values should be compared, the length of the wall (l_w) and $M_u/4V_u$, greater of the two will determine required height (Figure 4.3). The comparison is given in Table 4.4, and it is concluded that transverse reinforcement of the boundaries of the wall sections from the base to a height equals to 88.58 in. (2250 mm, corresponds to the first-floor walls only) should satisfy the SBE requirements.

Table 4.5 Required Length of the SBEs

	l_w (in.)	M_u (kip-ft)	V_u (kip)	$M_u/4V_u$ (in.)
Inner Walls	88.58	1371.77	51.19	80.39
Corner Walls	88.58	1466.85	54.78	80.33

It can be seen from Figure 4.3 that the width of the flexural compression zone (b) should be at least $h_u/16$ (h_u is the laterally unsupported height at extreme compression fiber of the wall) or if c/l_w is bigger than 3/8 than b should be at least 12 inches. It is found that the b should be at least 5.73 in. Since the widths of the walls are 9.06 in (230 mm), this provision is satisfied.

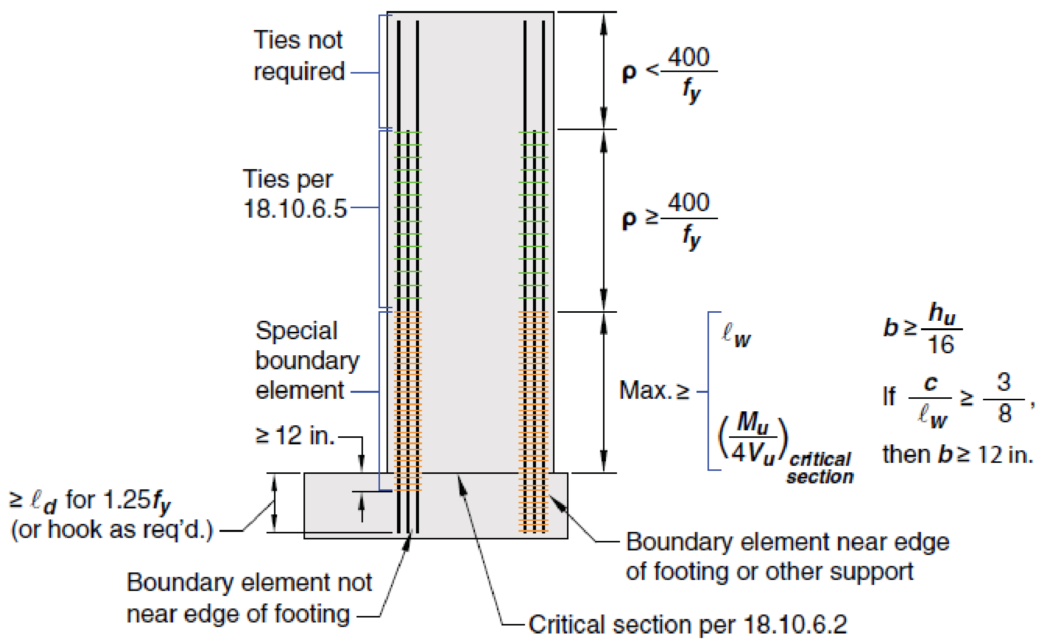

Figure 4.3 Boundary element requirements of the walls [1]

Figure 4.4 summarizes the requirements that the transverse reinforcement of the special boundary elements must satisfy. Based on the given requirements, length of boundary elements (l_{be}), maximum center-to-center spacing of longitudinal bars that are laterally supported (h_x), center-to-center spacing of transverse reinforcements (s) and the total amount of transverse reinforcement in the boundary element (A_{sh}) in the x- and y-directions are compared with actual experimental values in Table 4.6. It is found that while the l_{be} and h_x requirements are satisfied, the spacing of the transverse reinforcement (s = 100 mm) is higher than the ACI 318-19 requirement (s_{req} = 76 mm). Also, the total amounts of transverse reinforcement (A_{sh}) are 41% and 47% of the minimum required values in the x- and y-direction, respectively (shown in red in Table 4.6).

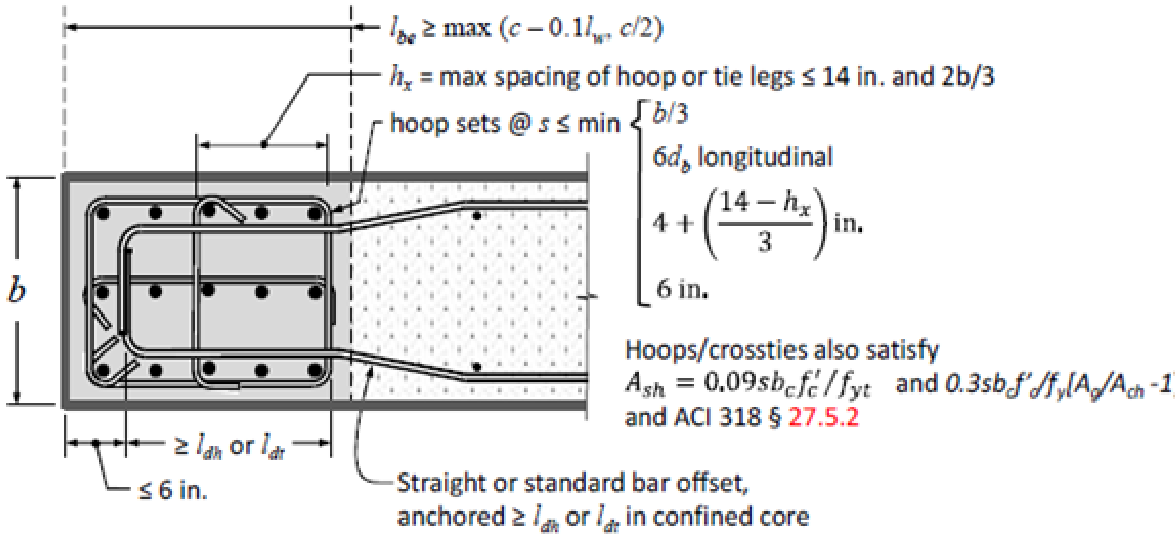

Figure 4.4 Requirements on the Transverse Reinforcement of Special Boundary Elements [6]

Table 4.6 Comparison of Transverse Reinforcement of the SBEs

	Used	Required
l_{be} (in.)	16.54	6.62
h_x (in.)	4.61	6.04
s (in.)	3.94	3.02
$A_{sh\text{-}x}$ (in.^{2})	0.49	1.18
$A_{sh\text{-}y}$ (in.^{2})	0.24	0.51

As mentioned before, wall boundaries extending from the base to a height of 2250 mm must satisfy the SBE requirements. Boundary elements above that (walls between the 2nd floor and the 8th floor) were checked to find if ordinary boundary element (OBE) provisions are required per §18.10.6.5 where it is stated that if the maximum longitudinal reinforcement ratio (ρ_l) at the wall boundary exceeds $400/f_y$ (Figure 4.3), OBE requirements must be satisfied. Table 4.7 shows the check if OBEs are required or not.

Table 4.7 Check on the Requirement of OBEs

	ρ_l	$400/f_y$
F2	0.022	0.008
F3	0.016	0.008
F4	0.016	0.008
F5	0.016	0.008
F6	0.016	0.008
F7	0.016	0.008

Based on Table 4.7, it is found that the boundary elements of the walls extending between the second floor and the 8th floor must satisfy the OBE requirements given in Figure 4.5. Summary of the required checks are given in Table 4.8. Although the SBEs over the first story do not satisfy the ACI 318-19 detailing requirements, OBEs at the upper stories are found to be compatible with §18.10.6.

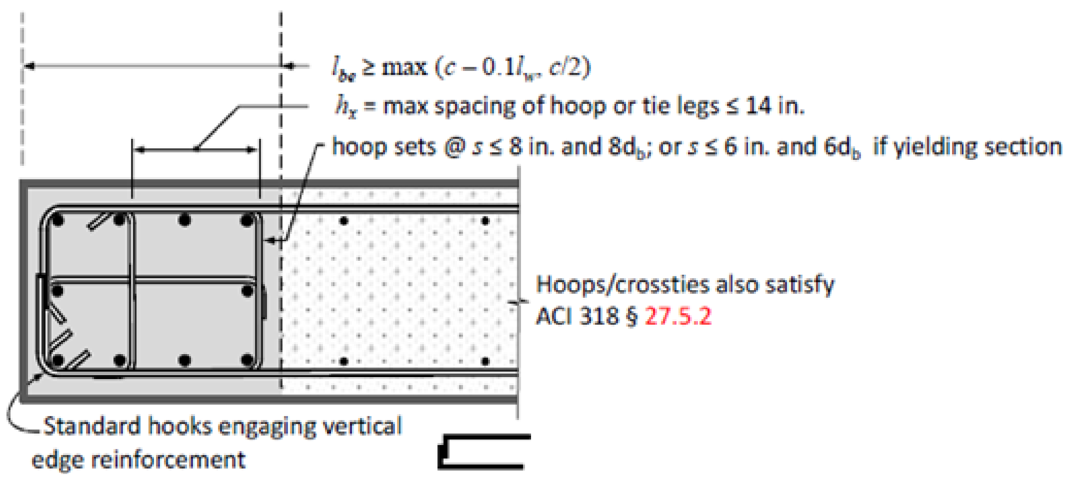

Figure 4.5 Requirements on the Transverse Reinforcement of Ordinary Boundary Elements [6]

Table 4.8 Comparison of Transverse Reinforcement of the OBEs

	Used	Required
l_{be} (in.)	16.54	6.62
h_x (in.)	13.82	14.00
s (in.)	3.94	5.98

Story drift ratios of the Building #1 in the wall direction are calculated by taking the redundancy factor in Equation 3.3 as 1.0. The calculated ratios are compared with the ASCE 7-16's maximum allowable story drift ratio (Δ_a) which is 0.02 for the reinforced concrete shear wall structures that are assigned to Risk Category I. Figure 4.6 shows the inter-story drift ratios of Building #1 in the wall direction.

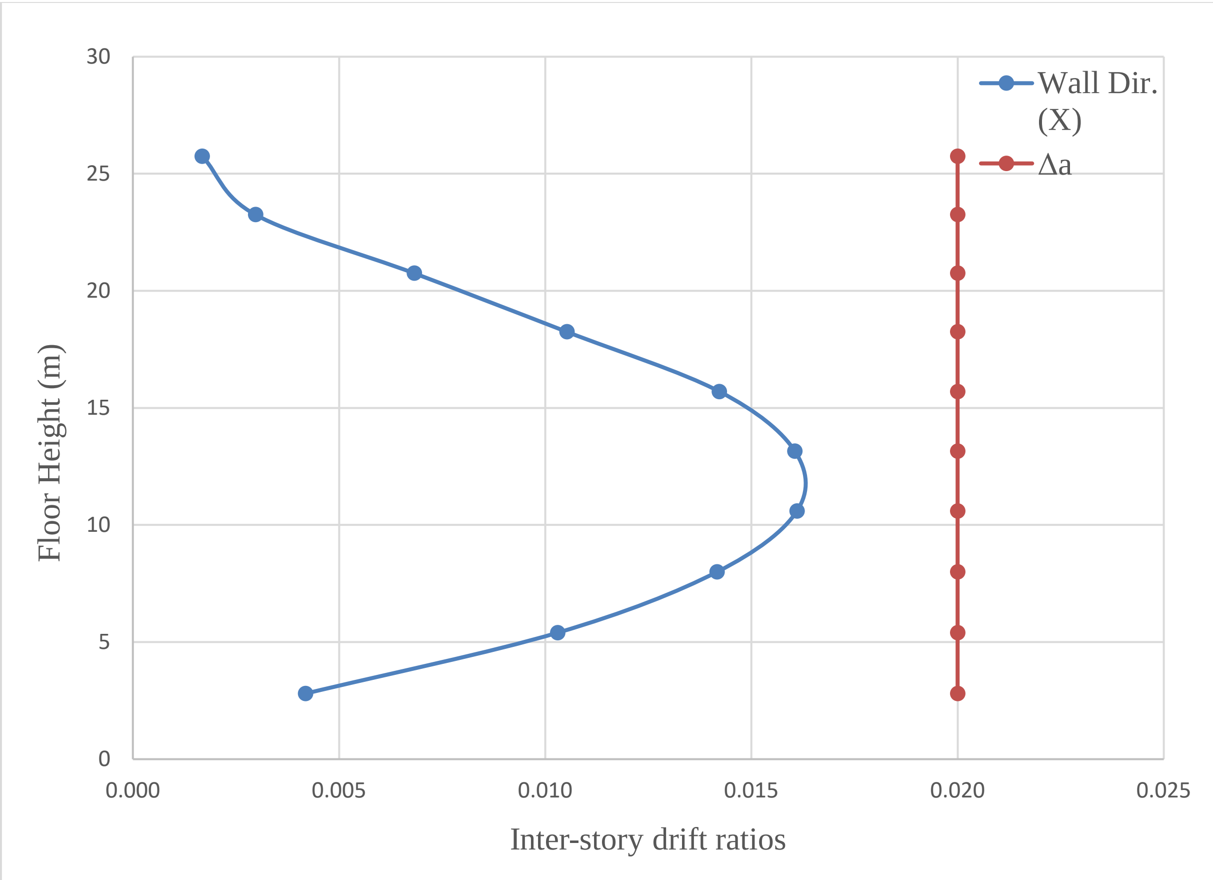

Figure 4.6 Story Drift Ratios in the Wall Direction

4.2 Columns

The lateral force resisting system of the test structure in the y-direction consists of 3 bay special reinforced concrete moment frames (R=8, Cd=5.5). Section sizes and the reinforcement details of the corner columns (C1) and the perimeter columns (C2) are given in Table 2.1 and Figure 2.3 respectively.

Similar to the shear walls, factored axial force-moment (ϕP-ϕM) capacity of the columns are calculated and compared with the demands that are calculated using the analysis procedure and loading conditions given in Chapter 3.

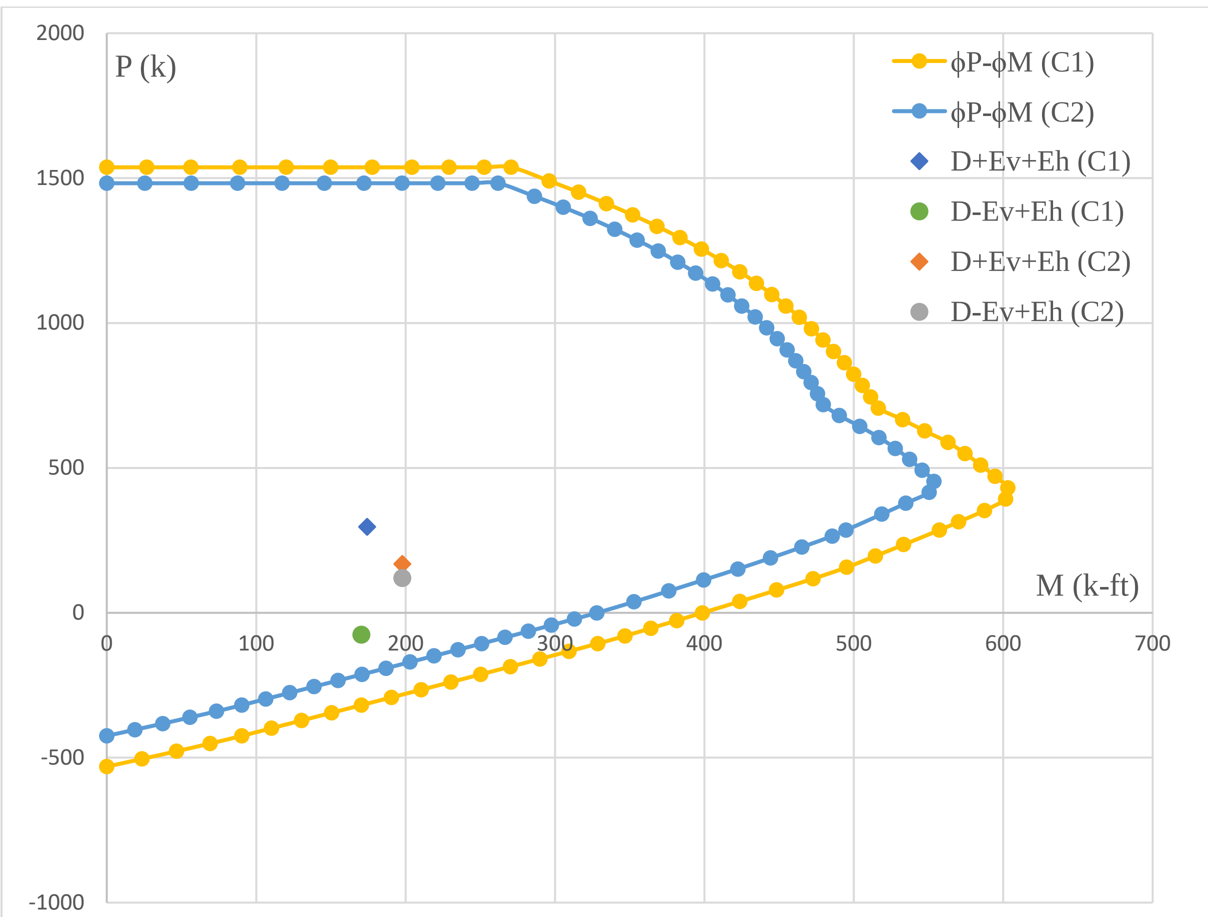

Figure 4.7 ϕP-ϕM Interaction Diagram of First Floor Columns with the demands

Figure 4.7 shows the ϕP-ϕM interaction diagrams of the first floor C1 and C2 columns, and the demands resulting from different load combinations at the base of the columns. It can be seen from the figure that axial force-moment demands are less than capacity of the columns. For the corner columns (C1), maximum resulting axial force, P_u = 296 kips (1317 kN), at the base of the columns is 10% of the total axial load capacity [1317 kN / (550 mm) (550 mm) (42 MPa) = 0.1]. This ratio decreases to 6% for the C2 columns [747 kN / (550 mm) (550 mm) (42 MPa) = 0.058]. Comparison of the demands on the columns with their ϕP-ϕM interaction diagrams are done for the upper stories too and it is concluded that all the columns in Building #1 satisfy the factored P-M capacity.

Amount and the detailing requirements of the transverse reinforcement of the columns are checked in accordance with ACI 318-19 §18.7.5. Spacing (*s*) requirements of the transverse reinforcement of the columns are summarized in Figure 4.8, and the comparison between the required and provided spacing values are given in Table 4.9 where it is shown that provided spacing of the columns' transverse reinforcement satisfy ACI 318-19.

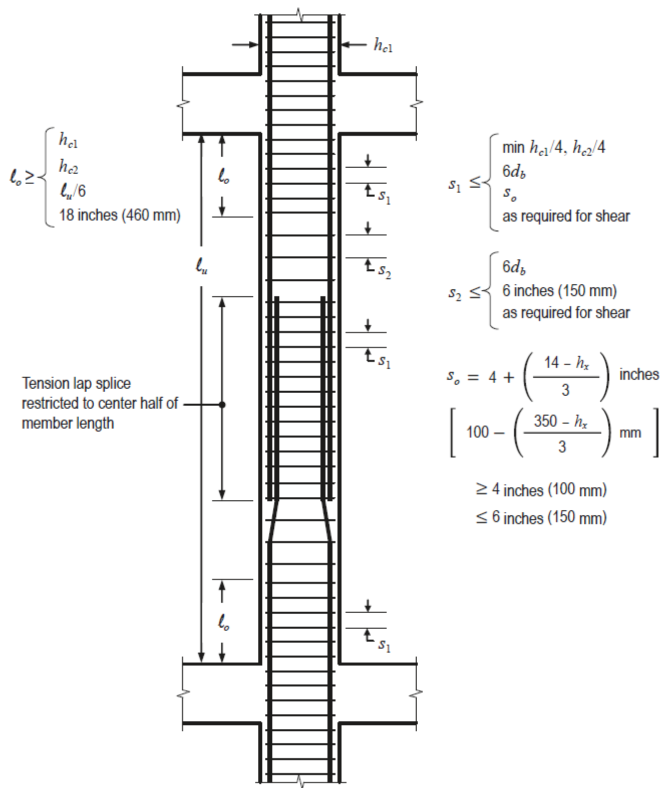

Figure 4.8 Column transverse reinforcement spacing requirements [8]

Table 4.9 Provided versus Required spacing of column transverse reinforcement

		Provided (mm)	Required (mm)	
		s_1-s_2	s_1	s_2
Floor 1	C1-C2	100	132	132
2^{nd} - 10^{th} Floors	C1-C2	100	102	132

Maximum center-to-center spacing of longitudinal bars laterally supported by crossties or hoop legs (h_x) is dependent on the amount of axial force (P_u) that the columns are carrying. If P_u is greater than $0.3A_gf'_c$ then h_x shall not exceed 8 in., otherwise h_x shall be maximum of 14 in. Table 4.10 gives the maximum required and the provided values. It is found that, except for the first-floor columns, columns in Building #1 do not satisfy limits on h_x in ACI 318-19 (shown in red in Table 4.10).

Table 4.10 Assessment of h_x of columns

		$h_{x\text{-prov}}$ (mm)	$h_{x\text{-req.}}$ (mm)
Floor 1	C1	224	356
	C2	179	
Floor 2	C1	448	
	C2	398	
3^{rd}-7^{th} Floors	C1	398	
	C2	398	
8^{th}, 9^{th} and 10^{th} Floors	C1	401	
	C2	401	

Total required cross-sectional areas of the transverse reinforcement ($A_{sh,req.}$) in the x- and y-directions of the columns are calculated based on the two following equations,

$$\frac{A_{sh}}{sb_c} \geq 0.3\left(\frac{A_g}{A_{ch}} - 1\right)\frac{f_c'}{f_{yt}} \tag{4.4}$$

$$\frac{A_{sh}}{sb_c} \geq 0.09\frac{f_c'}{f_{yt}} \tag{4.5}$$

where b_c is the cross-sectional dimension of the member core measured to the outside edges of the transverse reinforcement. Greater of the A_{sh} values from Equations 4.4 and 4.5 yielded in the minimum required total amount of transverse reinforcement to be used to satisfy ACI 318 provisions. Provided values are calculated based on the cross-section details of the columns given in Figure 2.3 and compared with the minimum requirements in Table 4.11.

Table 4.11 A_{sh} required versus provided

<table>
<tr><th rowspan="2"></th><th rowspan="2"></th><th colspan="2">Provided (mm^2)</th><th colspan="2">Required (mm^2)</th></tr>
<tr><th>$A_{sh,x}$</th><th>$A_{sh,y}$</th><th>$A_{sh,x}$</th><th>$A_{sh,y}$</th></tr>
<tr><td rowspan="2">Floor 1</td><td>C1</td><td rowspan="2">314</td><td rowspan="2">314</td><td rowspan="4">236</td><td rowspan="2">236</td></tr>
<tr><td>C2</td></tr>
<tr><td rowspan="2">Floor 2</td><td>C1</td><td rowspan="12">157</td><td>157</td><td rowspan="2">212</td></tr>
<tr><td>C2</td><td>314</td></tr>
<tr><td rowspan="2">Floors 3 and 4</td><td>C1</td><td>157</td><td rowspan="2">166</td><td rowspan="2">166</td></tr>
<tr><td>C2</td><td>314</td></tr>
<tr><td rowspan="2">Floor 5</td><td>C1</td><td>157</td><td>443</td><td>443</td></tr>
<tr><td>C2</td><td>314</td><td>166</td><td>166</td></tr>
<tr><td rowspan="2">Floor 6</td><td>C1</td><td>157</td><td rowspan="6">362</td><td rowspan="6">362</td></tr>
<tr><td>C2</td><td>314</td></tr>
<tr><td rowspan="2">Floors 7 and 8</td><td>C1</td><td>157</td></tr>
<tr><td>C2</td><td>236</td></tr>
<tr><td rowspan="2">Floors 9 and 10</td><td>C1</td><td rowspan="2">157</td></tr>
<tr><td>C2</td></tr>
</table>

Based on the Table 4.11, it is concluded that first floor columns satisfy the A_{sh} requirement of ACI 318-19. However, for the upper stories, with the exceptions of 2nd, 3rd, 4th and 5th floor C2 columns in the y-direction, total cross-sectional area of the transverse reinforcement in the Building #1 columns are less than required (shown in red).

Nominal shear strength ($V_n = V_c + V_s$) of the columns are calculated in accordance with §22.5 and §18.7.6. Shear strength provided by the concrete (V_c) can be calculated from Equation (a) or (b) from Table 22.5.5.1 of ACI 318-19. In this study, following equation (Equation-a) is used,

$$V_c = (2\lambda\sqrt{f_c'} + \frac{N_u}{6A_g})b_w d \tag{4.6}$$

It is important to mention that in accordance with §18.7.6, V_c is taken as zero over lengths l_0 (Figure 4.2.2) if the earthquake-induced shear force is at least one-half of the maximum required shear strength within l_0 and the factored axial compressive force (P_u) is less than $A_g f'_c/20$. Table 4.12 shows the calculated V_c, V_s and ϕV_n of the Building #1 columns over the length l_0 and at the middle of the columns.

Table 4.12 Shear strength of C1 and C2 columns

		l_0			middle		
		V_c (kips)	V_s (kips)	ϕV_n (kips)	V_c (kips)	V_s (kips)	ϕV_n (kips)
Floor 1	C1	0.0	276.7	207.5	54.5	276.7	248.4
	C2	0.0	276.7	207.5	84.1	276.7	270.6
Floor 2	C1	0.0	124.5	93.3	50.7	124.5	131.4
	C2	0.0	248.9	186.7	75.3	248.9	243.1
Floor 3	C1	0.0	124.5	93.3	41.9	124.5	124.8
	C2	0.0	248.9	186.7	61.5	248.9	232.8
Floor 4	C1	0.0	124.5	93.3	44.5	124.5	126.8
	C2	0.0	248.9	186.7	59.6	248.9	231.4
Floor 5	C1	0.0	46.8	35.1	46.9	46.8	70.2
	C2	0.0	248.9	186.7	57.8	248.9	230.1
Floor 6	C1	0.0	46.8	35.1	44.2	46.8	68.2
	C2	0.0	93.5	70.2	51.6	93.5	108.9
Floor 7	C1	0.0	46.8	35.1	45.4	46.8	69.1
	C2	0.0	70.2	52.6	49.7	70.2	89.9
Floor 8	C1	0.0	46.9	35.2	45.9	46.9	69.7
	C2	0.0	70.4	52.8	48.6	70.4	89.2
Floor 9	C1	0.0	46.9	35.2	45.7	46.9	69.4
	C2	0.0	46.9	35.2	46.9	46.9	70.4
Floor 10	C1	0.0	46.9	35.2	44.7	46.9	68.7
	C2	0.0	46.9	35.2	45.1	46.9	69.1

The design shear force (V_e) is calculated from considering the maximum forces that can be generated at the faces of the joints at each end of columns. These joint forces are calculated using the maximum probable flexural strengths (M_{pr}) at each end of the column associated with the range of factored axial forces acting on the column. A maximum limit point is set where the column shears did not exceed those calculated from joint strengths based on M_{pr} of the beams framing into the joint. For the M_{pr} of the beams, T-beam configuration is assumed and the longitudinal slab reinforcements in the effective flange widths are included in the calculations. Table 4.13 shows the calculated design shear forces of columns C1 and C2.

Table 4.13 Design shear forces

		V_e (kips)
Floor 1	C1	73.9
	C2	96.5
Floor 2	C1	77.5
	C2	101.2
Floor 3	C1	77.5
	C2	101.2
Floor 4	C1	70.4
	C2	91.8
Floor 5	C1	51.6
	C2	91.8
Floor 6	C1	43.7
	C2	85.9
Floor 7	C1	39.2
	C2	83.0
Floor 8	C1	29.3
	C2	59.6
Floor 9	C1	24.5
	C2	54.0
Floor 10	C1	24.5
	C2	48.3

Finally, the factored shear strength (ϕV_n) of columns is compared with the design shear forces (V_e) in Table 4.14. It is concluded that the shear demand on most of the Building #1's C1 and C2 columns are less than the shear strength. However, shear failures are predicted at the ends (over the length l_0) of 5th floor C1 columns, 6th and 7th floors C1 and C2 columns, and C2 columns of the 8th, 9th and the 10th stories where V_e / ϕV_n ratios are higher than unity (shown in red in Table 4.14).

Table 4.14 Assessment of shear strength of columns

V_e / ϕV_n		l_0	middle
Floor 1	C1	0.36	0.30
	C2	0.46	0.36
Floor 2	C1	0.83	0.59
	C2	0.54	0.42
Floor 3	C1	0.83	0.62
	C2	0.54	0.43
Floor 4	C1	0.75	0.56
	C2	0.49	0.40
Floor 5	C1	1.47	0.74
	C2	0.49	0.40
Floor 6	C1	1.25	0.64
	C2	1.22	0.79
Floor 7	C1	1.12	0.57
	C2	1.58	0.92
Floor 8	C1	0.83	0.42
	C2	1.13	0.67
Floor 9	C1	0.70	0.35
	C2	1.53	0.77
Floor 10	C1	0.70	0.36
	C2	1.37	0.70

Inter-story drift ratios of the Building #1 in the moment-frame direction (y dir.) are also calculated by taking the redundancy factor in Equation 3.3 as 1.0. The calculated ratios are compared with the ASCE 7-16's maximum allowable story drift ratio (Δ_a) which is 0.02 for the reinforced concrete moment frame structures that are assigned to Risk Category I. Figure 4.9 shows the inter-story drift ratios of Building #1 in the y direction.

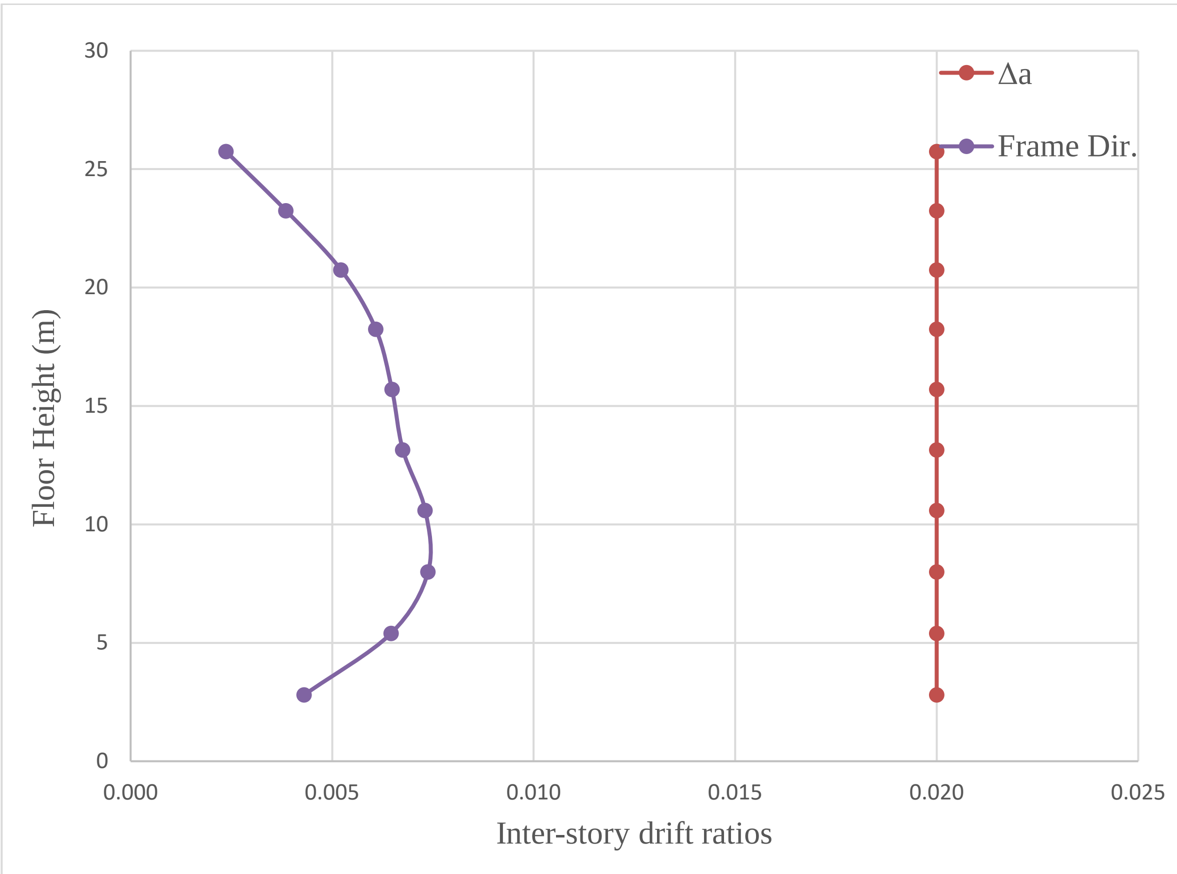

Figure 4.9 Story Drift Ratios in the Moment-Frame Direction

4.3 Beams

Flexural strength of the beams is calculated using T-beam assumption based on the effective flange widths calculated in accordance with ACI 318-19 Table 6.3.2.1. In terms of the longitudinal reinforcement, G1 and G3 beams were divided into 3 different parts, outer end (1.4 meter away from the C1 columns), inner end (1.4 meter away from the C2 columns) and the center. Accordingly, G2 beams have two different regions (ends and center). Reinforcement details of the beams are given in Figure 2.4. Table 4.15 shows the ratio of factored flexural capacities (ϕM_n) of the perimeter beams to the moment demands (M_u) for both the positive and negative moments occurring at the different parts of the beams. Results showed that for all the perimeter beams in Building #1 the flexural demands are lower than the capacities both under positive and negative moments with a highest $M_u/\phi M_n$ ratio of 0.87 at the 3rd floor G1 (or G3) beams inner end.

Table 4.15 Moment demands divided by the moment capacities for the G1-G3 and G2 beams

$M_u/\phi M_n$		G1 and G3			G2	
		Outer	Center	Inner	Ends	Center
2nd Floor	+	0.67	0.28	0.83	0.52	0.21
	-	0.64	0.19	0.72	0.57	0.12
3rd Floor	+	0.70	0.29	0.87	0.58	0.22
	-	0.67	0.21	0.76	0.62	0.14
4th Floor	+	0.69	0.28	0.82	0.59	0.18
	-	0.73	0.20	0.72	0.52	0.11
5th Floor	+	0.75	0.26	0.77	0.57	0.18
	-	0.67	0.19	0.79	0.50	0.10
6th Floor	+	0.66	0.25	0.85	0.53	0.17
	-	0.61	0.17	0.72	0.46	0.09
7th Floor	+	0.57	0.24	0.72	0.47	0.17
	-	0.63	0.13	0.63	0.49	0.07
8th Floor	+	0.53	0.20	0.68	0.56	0.19
	-	0.52	0.07	0.60	0.50	0.05
9th Floor	+	0.48	0.16	0.48	0.56	0.15
	-	0.46	0.05	0.46	0.46	0.04
10th Floor	+	0.25	0.12	0.26	0.38	0.13
	-	0.31	0.01	0.36	0.40	0.01
Roof	+	0.12	0.12	0.12	0.17	0.11
	-	0.16	0.02	0.16	0.24	0.02

Moment capacities of the beams are then compared with moment capacities of the columns. According to ACI 318-19 §18.7.3.2, sum of the nominal flexural strength of columns ($\sum M_{nc}$) framing into a joint must be at least 1.2 times the sum of the nominal flexural strength of the beams ($\sum M_{nb}$) framing into the same joint. Table 4.16 shows the ratio $\sum M_{nc}$ / $\sum M_{nb}$ for both of the load combinations (Equations 3.1 and 3.2), for lateral loads applied at +y and –y directions, and for the Joint 1 (where G1-G3 beams framing into C1 columns) and Joint 2 (where G1-G3 and G2 beams framing into C2 columns). For the Joint 1, results are shown until the 5th floor due to the fact that until the 5th floor CG1 beams are used at the overhanging slab. Since after the 5th floor, only the G1 (or G3) beams are framing into the Joint 1, $\sum M_{nc}$ / $\sum M_{nb}$ ratio is not checked. Results indicate ratios lower than ACI 318-19 requirement (1.2) at the 3rd and 7th floor Joint 2 and 4th floor Joint 1 under the second load case and in the sway direction of +Y (shown in red in Table 4.16). In general, column to beam moment strength ratios are around 1.20-1.35 for Joint 2 and ranging from 1.16 to 2.67 for Joint 1.

Table 4.16 Strong Column – Weak Beam assessment

$\frac{\sum Mnc}{\sum Mnb}$	Joint 1				Joint 2			
	$D + E_v + E_h$		$D - E_v + E_h$		$D + E_v + E_h$		$D - E_v + E_h$	
	Sway +Y	Sway -Y	Sway +Y	Sway -Y	Sway +Y	Sway -Y	Sway +Y	Sway -Y
Floor 2	1.97	2.67	1.86	2.60	1.51	1.67	1.41	1.57
Floor 3	1.47	2.05	1.38	1.98	1.22	1.36	1.14	1.27
Floor 4	1.25	1.82	1.16	1.75	1.29	1.32	1.21	1.24
Floor 5	-	-	-	-	1.36	1.30	1.29	1.23
Floor 6	-	-	-	-	1.31	1.38	1.25	1.31
Floor 7	-	-	-	-	1.20	1.38	1.15	1.32
Floor 8	-	-	-	-	1.35	1.43	1.28	1.36
Floor 9	-	-	-	-	1.27	1.32	1.22	1.26
Floor 10	-	-	-	-	1.34	1.37	1.31	1.34

Transverse reinforcement detailing of the beams is summarized in Figure 4.10 where the maximum allowable spacing of the transverse reinforcement is shown differently for the different parts of the beam; spacing along 2 times the beam height (h_b) away from the joint faces, spacing at the lap splices and the spacing in between the two.

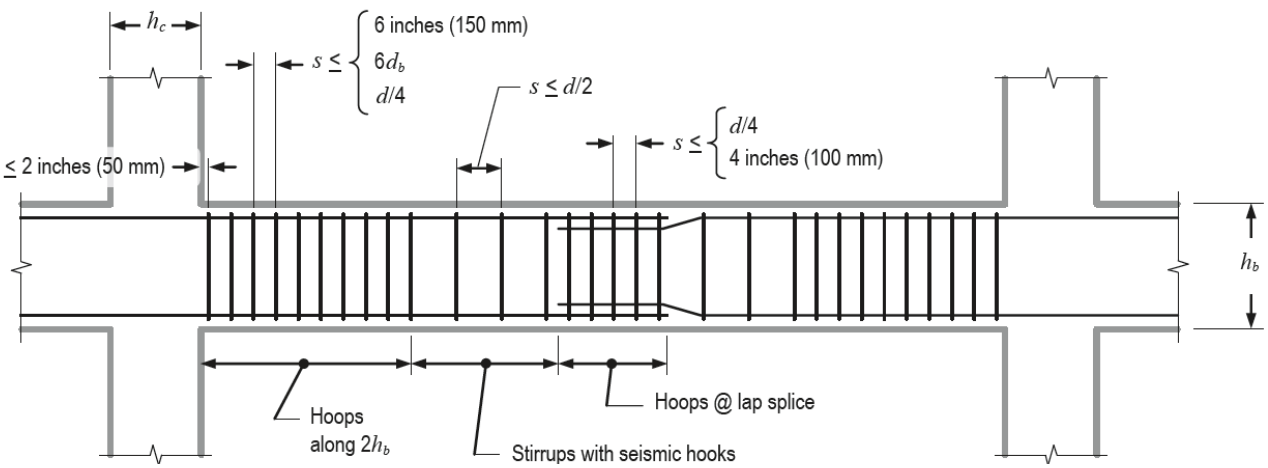

Figure 4.10 Spacing requirements of the beams [8]

Table 4.17 shows the comparison between the transverse reinforcement spacing of the beams and the required values based on Figure 4.10. Although the provided amount of spacing satisfies the ACI 318 requirements at the parts of the beams where there are no lap splices and at least $2h_b$ away from the joint face, beams of 6th floor through roof do not satisfy the requirements at the beam ends and at the parts with the splices (shown in red in Table 4.17).

Table 4.17 Spacing of the transverse reinforcement of the beams

		Provided (mm)	Required (mm)		
			along $2h_b$	in between	at lab splice
Story 2	G1/G3	100	118.5	237.0	100.0
	G2	100	118.5	237.0	100.0
Story 3	G1/G3	100	118.5	237.0	100.0
	G2	100	118.5	237.0	100.0
Story 4	G1/G3	100	118.5	237.0	100.0
	G2	100	118.5	237.0	100.0
Story 5	G1/G3	125	118.5	237.0	100.0
	G2	100	118.5	237.0	100.0
Story 6	G1/G3	150	118.5	237.0	100.0
	G2	125	118.5	237.0	100.0
Story 7	G1/G3	200	118.5	237.0	100.0
	G2	175	118.5	237.0	100.0
Story 8	G1/G3	200	106.4	212.7	100.0
	G2	150	106.4	212.7	100.0
Story 9	G1/G3	200	106.4	212.7	100.0
	G2	200	106.4	212.7	100.0
Story 10	G1/G3	200	106.4	212.7	100.0
	G2	200	106.4	212.7	100.0
Roof	G1/G3	200	106.4	212.7	100.0
	G2	200	106.4	212.7	100.0

Shear strength of the beams are calculated in accordance with ACI 318-19 §18.6.5 and §22.5. For the calculation of shear strength of the concrete (V_c) Equation 4.6 is used with $N_u = 0$. Similar to columns, V_c is taken as zero at the ends of the beams ($2h_b$ away from the joint faces) where the earthquake-induced shear force represents at least one-half of the maximum required shear strength. Table 4.18 shows the factored shear strength of the G1/G3 and G2 beams at the mid-span of the beams and along $2h_b$ away from the joint faces.

Table 4.18 Factored shear strength of the beams

ϕV_n (kips)		G1/G3	G2
2nd Floor	along $2h_b$	37.03	37.03
	mid-span	67.14	67.14
3rd Floor	along $2h_b$	37.03	37.03
	mid-span	67.14	67.14
4th Floor	along $2h_b$	37.03	37.03
	mid-span	63.72	63.72
5th Floor	along $2h_b$	29.63	37.03
	mid-span	56.31	63.72
6th Floor	along $2h_b$	24.69	29.63
	mid-span	51.37	56.31
7th Floor	along $2h_b$	18.52	21.16
	mid-span	42.65	45.30
8th Floor	along $2h_b$	16.62	22.16
	mid-span	35.19	40.74
9th Floor	along $2h_b$	16.62	16.62
	mid-span	35.19	35.19
10th Floor	along $2h_b$	16.62	16.62
	mid-span	35.19	35.19
Roof	along $2h_b$	16.62	16.62
	mid-span	35.19	35.19

For the calculation of the shear demands, the design shear force (V_e) is calculated by considering the forces on the portion of the beam between the faces of the joints. It is assumed that the moments of opposite sign corresponding to probable flexural strength (M_{pr}) act at the joint faces and that the beam is loaded with the gravity and vertical earthquake loads along its span ($w_u = D+0.2S_{ds}D$), refer to Figure 4.11.

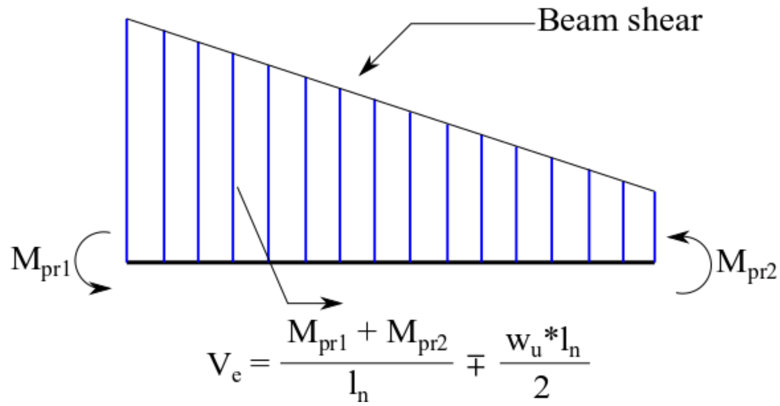

Figure 4.11 Design shear force distribution for the beams

Table 4.19 shows the calculated design shear forces at the mid-span of the beams and at the faces of the joints.

Table 4.19 Design shear forces of the beams

V_e (kips)		G1/G3	G2
2nd Floor	at joint face	65.32	64.22
	at mid-span	57.87	56.77
3rd Floor	at joint face	64.20	63.11
	at mid-span	57.44	56.35
4th Floor	at joint face	62.17	57.45
	at mid-span	55.57	50.85
5th Floor	at joint face	56.89	57.37
	at mid-span	50.43	50.91
6th Floor	at joint face	52.94	57.42
	at mid-span	46.40	50.88
7th Floor	at joint face	52.64	52.64
	at mid-span	44.76	44.76
8th Floor	at joint face	38.17	41.07
	at mid-span	32.15	35.05
9th Floor	at joint face	34.65	34.65
	at mid-span	28.45	28.45
10th Floor	at joint face	34.29	31.38
	at mid-span	28.09	25.18
Roof	at joint face	30.97	30.97
	at mid-span	25.44	25.44

Finally, Tables 4.18 and 4.19 are compared to calculate the shear demand to capacity ratios ($V_e/\phi V_n$). Results showed that the beams of Building #1 do not satisfy the minimum required shear strength over the parts $2h_b$ away from the joint faces and also at the 7th floor G1/G3 beams midspan (shown in red), Table 4.20.

Table 4.20 Shear demands versus shear capacity of the beams

$V_e/\phi V_n$ (kip)		G1/G3	G2
2nd Floor	along $2h_b$	1.76	1.73
	mid-span	0.86	0.85
3rd Floor	along $2h_b$	1.73	1.70
	mid-span	0.86	0.84
4th Floor	along $2h_b$	1.68	1.55
	mid-span	0.87	0.80
5th Floor	along $2h_b$	1.92	1.55
	mid-span	0.90	0.80
6th Floor	along $2h_b$	2.14	1.94
	mid-span	0.90	0.90
7th Floor	along $2h_b$	2.84	2.49
	mid-span	1.05	0.99
8th Floor	along $2h_b$	2.30	1.85
	mid-span	0.91	0.86
9th Floor	along $2h_b$	2.08	2.08
	mid-span	0.81	0.81
10th Floor	along $2h_b$	2.06	1.89
	mid-span	0.80	0.72
Roof	along $2h_b$	1.86	1.86
	mid-span	0.72	0.72

4.4 Beam-Column Joints

Beam-column joints of Building #1 are designed to have two legs of 10 mm in diameter transverse reinforcement with a spacing of 150 mm. Shear strength of the beam-column joints are calculated, in accordance with ASCE 41-17 [10] §10.4, based on the following generalized equation,

$$V_n = \gamma\lambda\sqrt{f_c'}A_j \tag{4.7}$$

where λ is taken as one for the normal-weight concrete. A_j is the effective cross-sectional area within the joint and it is calculated as the product of overall depth of column and the effective joint width. Effective joint width is taken as the lesser of i) beam width plus the column depth and ii) twice the perpendicular distance from longitudinal axis of beam to nearest side face of column. γ in Equation 4.7 represents a coefficient whose value is taken based on the configuration of the columns and beams framing into the joint, and the conformity of the transverse reinforcement in the joint. Table 10-12 of ASCE 41-17 provides the values for γ coefficient. Whether the joint transverse reinforcement can be considered as conforming or not is related to the spacing of the hoops. If the hoops are spaced at less than half of the depth of the column parallel to the longitudinal axis of the beam framing into the joint, joints are considered as confirming. Since the hoop spacing is 150 mm and the depth of the columns are 550 mm at the first story and 500 mm for the rest of the floors, confirming component values of γ in Table 10-12 are used. Overall, γ is taken as 15 for the Joint 2 for all of the stories. For Joint 1, while it is also 15 for the 2^{nd}, 3^{rd} and the 4^{th} floors, for the 5^{th} through 10^{th} floors γ=12. Table 4.21 shows the beams framing into the joints, the corresponding A_j values, conformity of the hoops (C is confirming and NC is non-conforming) and γ values.

Table 4.21 Joint effective cross-sectional areas and γ values based on ASCE 41-17

		Beams	*Aj* (in2)	Conformity	γ
2nd Floor	Joint 1	CG1-G1	468.9	C	15
	Joint 2	G1-G2		C	15
3rd Floor	Joint 1	CG1-G1	426.3	C	15
	Joint 2	G1-G2		C	15
4th Floor	Joint 1	CG1-G1	387.5	C	15
	Joint 2	G1-G2		C	15
5th -10th Floors	Joint 1	-G1	387.5	C	12
	Joint 2	G1-G2		C	15
Roof	Joint 1	-G1	387.5	C	8
	Joint 2	G1-G2		C	8

Shear demands occurring at the joints (V_u) are calculated on a plane at mid-height of the joint from calculated forces at the joint faces using tensile and compressive beam forces assuming that the stress in the flexural tensile reinforcement is $1.25f_y$ and column shear consistent with the beam nominal moment strengths (M_n) in accordance with ACI 318-19 §18.3.4. Figure 4.12 illustrates the forces that are used to calculate joint shear demands.

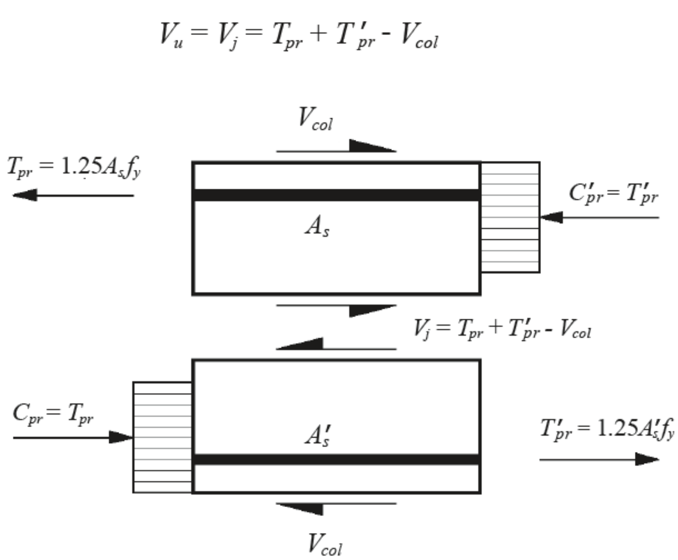

Figure 4.12 Joint shear free body diagram [8]

It is important to note here that the joint shear demands are calculated for the sway in +y and –y directions separately, and the greater of the two results are used for the assessment. Table 4.22 shows the ratio of calculated shear forces to factored joint shear strength.

Table 4.22 Joint shear assessment based on ASCE 41-17

$V_u/\phi V_n$	Joint 1	Joint 2
Story 2	0.51	0.63
Story 3	0.56	0.69
Story 4	0.61	0.77
Story 5	0.53	0.77
Story 6	0.53	0.67
Story 7	0.47	0.75
Story 8	0.44	0.56
Story 9	0.35	0.49
Story 10	0.35	0.41
Roof	0.29	0.55

Since diagonal shear cracks were reported at 3rd, 4th and 5th floor beam-column joints after the experiment (Chapter 2), $V_u/\phi V_n$ ratios less than unity in Table 4.22 indicate that current provisions of ASCE 41 cannot predict these failures. Therefore, a more detailed approach proposed by LaFave and Kim [5] is used for the calculation of beam-column joint shear strength. The proposed method not only incorporates the concrete compressive strength and joint cross-sectional area (as in Equation 4.7) but also uses the amount of transverse reinforcement in the joint and beam reinforcement ratio. The joint shear strength calculation given as follows,

$$V_n(N) = A_j(mm^2)\, \alpha_t \beta_t \eta_t \lambda_t (JI)^{0.15} (BI)^{0.30} (f_c')^{0.75} \tag{4.7}$$

while α_t is a parameter for in-plane geometry (1.0 for interior connections, 0.7 for exterior connections and 0.4 for knee connections), β_t is a parameter related with the out-of-plane geometry (1.0 for joints with 0 or 1 transverse beams and 1.18 for joints with 2 transverse beams). η_t describes the joint eccentricity with the equation $\eta_t = (1 - e/b_c)^{0.67}$ where e is the eccentricity between the beam and column centerlines. λ_t is taken as 1.31. *JI and BI* represent joint transverse reinforcement index (defined as $\rho_j \times f_{yj}/f'_c$ where ρ_j is the volumetric joint transverse reinforcement ratio) and beam reinforcement index (defined as $\rho_b \times f_{yb}/f'_c$ in which ρ_b is the beam reinforcement ratio) respectively. For the calculation of effective joint cross-sectional area, a different approach is used than the one proposed by ASCE 41. A_j is calculated based on the provisions of ACI 352R-02; the product of column depth times the average of beam and column width. Based on Equation 4.7, joint shear capacity is calculated and compared with the demands in Table 4.23 where it can be seen that this approach was able to predict the joint shear failure at the floors where the damage was observed after the experiments (shown in red in Table 4.23). Results indicate failure at Joint 2 of the roof.

Table 4.23 Joint shear assessment based on LaFave and Kim [5]

$Vu/\phi Vn$	Joint 1	Joint 2
Story 2	0.69	0.87
Story 3	0.75	0.95
Story 4	0.77	1.00
Story 5	0.79	1.00
Story 6	0.79	0.88
Story 7	0.70	0.97
Story 8	0.67	0.74
Story 9	0.56	0.69
Story 10	0.56	0.61
Roof	0.58	1.08

Another approach for the calculation of the joint shear strength is proposed by Hassan W. in his PhD dissertation [3]. The author balloted the following procedure to ACI 369M20 committee. A similar approach to the ASCE 41's method (Eqn. 4.7) was proposed with two main changes. First, whether the transverse reinforcement of the joints is confirming or not was suggested to be determined by the following equation, $s \leq h_k/3$, where h_k is the depth of the column core. Second, instead of using a predefined constant of γ for the non-conforming joints, its value is determined based on the joint aspect ratio and the axial load. For example, the γ coefficient of Joint 2 of the Building #1 is calculated by the following formula $13\sqrt{\frac{h_c}{h_b}}\kappa_{js}$ (compared to a constant value of 15, Table 4.21), where κ_{js} is the axial load factor and it is permitted to be taken as 1.0. Based on these provisions, a similar table to Table 4.21 is constructed and given below. It should be noted here that similar to LaFave and Kim, Hassan W. also proposed the usage of ACI 352R-02 formula for the calculation of effective joint width which resulted in average of beam and column width (its value was the column width for the ASCE 41-17 approach).

Table 4.24 Joint effective cross-sectional areas and γ values based on Hassan [3]

		Beams	*Aj* (in2)	Conformity	γ
2nd Floor	Joint 1	CG1-G1	383.6	C	15.0
	Joint 2	G1-G2		C	15.0
3rd Floor	Joint 1	CG1-G1	348.8	NC	12.4
	Joint 2	G1-G2		NC	12.4
4th Floor	Joint 1	CG1-G1	329.4	NC	12.4
	Joint 2	G1-G2		NC	12.4
5th, 6th and 7th Floors	Joint 1	G1	329.4	NC	10.5
	Joint 2	G1-G2		NC	12.4
8th, 9th and 10th Floors	Joint 1	G1	310.0	NC	11.0
	Joint 2	G1-G2		NC	13.0
Roof	Joint 1	G1	310.0	NC	4.0
	Joint 2	G1-G2		NC	4.0

Comparison of Tables 4.21 and 4.24 shows that unlike the ASCE 41, proposed approach suggests that the transverse reinforcement of the joints of Building #1 (except the second-floor joints) are non-confirming. The joint shear demands are calculated as explained before (Figure 4.12) and compared with the capacities in Table 4.25. The comparison shows that the method proposed by Hassan W. is able to predict the joint shear failures observed after the experiment.

Table 4.25 Joint shear assessment based on Hassan [3]

$Vu/\phi Vn$	Joint 1	Joint 2
Story 2	0.62	0.77
Story 3	0.83	1.02
Story 4	0.87	1.09
Story 5	0.72	1.09
Story 6	0.72	0.96
Story 7	0.64	1.06
Story 8	0.61	0.81
Story 9	0.47	0.70
Story 10	0.47	0.59
Roof	0.73	1.36

CHAPTER 5. ASSESSMENT OF 2018 TEST STRUCTURE

This chapter focuses on the assessment of 2018 test structure (Building #2) using the ACI 318-19 provisions where the member section dimensions and the column reinforcement details of the structure are given in Table 2.4, Figures 2.3 and 2.4 respectively. The model and the loading conditions used to calculate the demands are explained in Chapter 3.

5.1 Shear Walls

Similar to Building #1, the lateral force resisting system of the structure in the x direction consists of 4 identical 2250 mm long special reinforced concrete shear walls. When they are compared with the Building #1 shear walls, it is observed that the thickness of the wall webs decreases to 150 mm from 230 mm for the 1st-6th floor walls and to 120 mm from 150 mm at the 7th floor. Walls are constructed to be continuous from the base of the structure to the 8th floor (for the upper three stories moment frames are used in each of the directions). Therefore, the total height of the walls are 18.25 meters (59.87*ft*). Figure 5.1 shows the cross-sections of the walls at the first floor (W15B), at the second floor (W15A) and at the 3rd through 6th floors (W15), and at the 7th floor (W12).

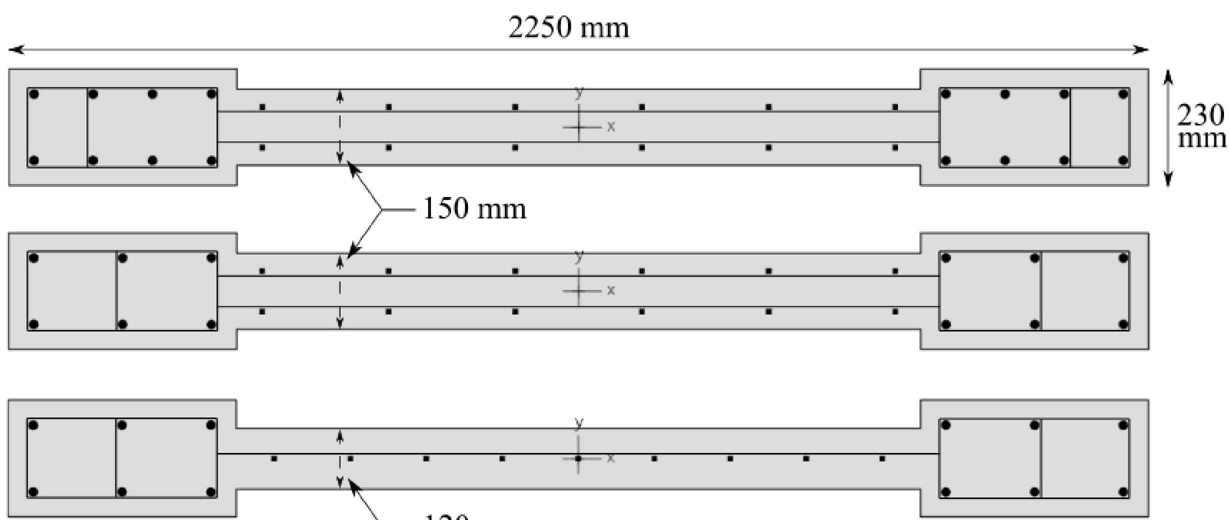

Figure 5.1 W15B (Top), W15A and W15 (Middle), W12 (Bottom) walls

Axial force and moment demands on the shear walls are compared with the wall capacities using the P-M interaction diagrams. This comparison is done for the all the shear walls in the structure but only the first story ϕP-ϕM diagram and demands are given in Figure 5.2 as an example.

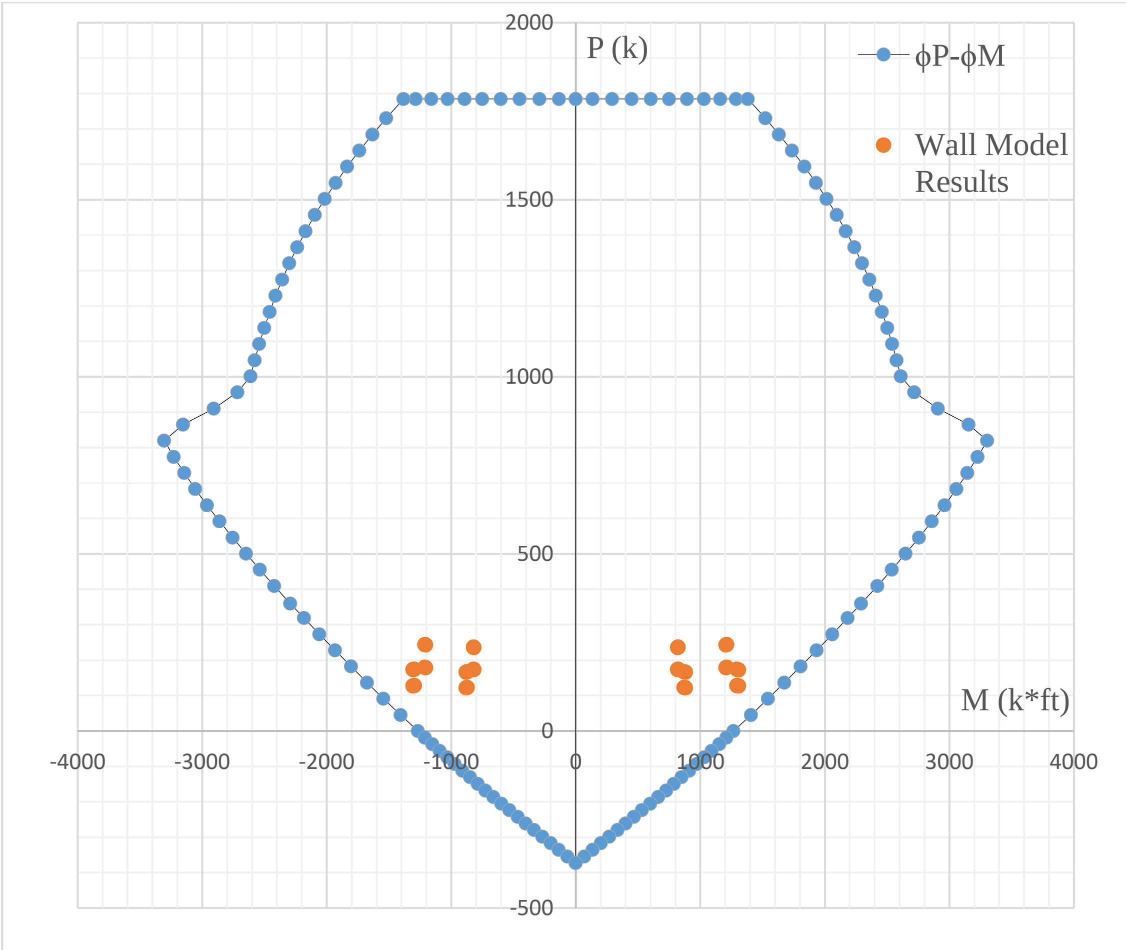

Figure 5.2 ϕP-ϕM diagram of the W15B walls and the corresponding demands

It can be observed from Figure 5.2 that the maximum axial load demand (P_u), corresponding to the first load combination (Eqn. 3.1), is almost 14% of the factored axial load capacity (ϕP_n) of the first story walls, [243*k* / (1784*k*) = 0.136]. Maximum bending moment is observed at the base of the corner walls with a value of 1308 *k*ft* which is 79% of the factored moment capacity under the same amount of axial load, [1308 *k*ft* / 1650 *k*ft* = 0.79].

Shear strength of the walls (V_n) are calculated in accordance with ACI 318-19 §18.10.4. The procedure for the calculation of the design shear force (V_e) and V_n are explained in Chapter 4.1. It should be noted here that due to the high values of the M_{pr}/M_u ratio, the overstrength factor Ω_v in Eqn. 4.2 is found to be around between 3.25 to 10. Therefore, for all the shear walls, maximum limiting value of $3V_u$ for V_e governs (see Eqn. 4.2). Table 5.1 shows the factored shear strength, design shear force and the ratio of the two, $V_e/\phi V_n$, which concludes that unlike the Building #1, 7th floor structural walls (shown in red in Table 5.1) do not satisfy ACI 318 shear strength provisions.

Table 5.1 Shear strength assessment of the walls

	ϕV_n (kips)	V_e (kips)	$V_e/\phi V_n$
F1	199.65	138.32	0.69
F2	165.56	115.48	0.70
F3-4-5	124.60	118.34	0.95
F6	119.42	79.87	0.67
F7	97.88	98.47	1.01

ACI 318-19's minimum distributed web reinforcement ratios, ρ_l and ρ_t, are defined as 0.0025 (§18.10.2.1). Calculations showed that these minimum ratios are satisfied at every level. $\rho_{l,min}$ within $0.15l_w$ from the end of a vertical wall segment is also set to the ratio of $6\sqrt{f_c'}/f_y$ (§ 18.10.2.4a). The minimum required amount and the used values are compared in Table 5.2.

Table 5.2 Comparison of ρ_l within 0.15lw

18.10.2.4a	$0.15\ l_w$ (mm)	337.5	
	$6\sqrt{f_c'}/f_y$	# bars in $0.15\ l_w$	ρ_l
F1	0.011	6	0.022
F2	0.011	4	0.015
F3-4-5	0.010	4	0.015
F6-7	0.009	4	0.015

Also, at least two curtains of reinforcement shall be used in the wall web if $V_u > 2\lambda\sqrt{f_c'}A_{cv}$ (§18.10.2.2). Table 5.3 shows the comparison between the required and used number of vertical reinforcement curtains and it is shown that 7th floor walls do not satisfy this requirement (shown in red).

Table 5.3 Required and used number of reinforcement curtains

Number of Curtains	Required	Used
F1	2	2
F2	2	2
F3-4-5	2	2
F6	2	2
F7	2	1

To be able to check if the special boundary element (SBE) provisions of ACI 318 are required or not, the largest neutral axis depth (c) corresponding to factored axial force in the direction of design displacement (δ_u) is calculated and compared with δ_u (Eqn. 4.4). For the calculation of δ_u, elastic displacements at the top of walls are obtained from the elastic analysis and then multiplied with C_d/I_e (5/1). Results showed that while the ratio $1.5\delta_u/h_w$ is around 0.023, $l_w/600c$ is found to be 0.013. Therefore, boundaries of the Building #2 must also satisfy the SBE requirements. How long the SBE's of the walls should extend vertically from the critical section is obtained by the greater of the two, l_w and $M_u/4V_u$, which yielded that wall boundaries from the base up to a 2250 mm height should be designed as SBEs. The first check on the SBE provisions is done on the width of the flexural compression zone, b, which must be greater than $h_u/16$ and 12 inches if c/l_w is greater than 3/8. Table 5.4 shows the required and the provided minimum compression zone widths which shows that boundaries of the first-floor walls satisfy this condition (shown in green).

Table 5.4 Assessment of width of flexural compression zone

	b_{req} (in.)	h_u (in.)	c (in.)	l_w (in.)	b_{used} (in.)
Corner Walls	5.78	92.52	11.20	88.58	9.06
Inner Walls	5.78	92.52	12.57	88.58	9.06

Figure 4.4 in Chapter 4.1 summarizes the requirements of ACI 318's on the transverse reinforcement of the wall boundaries such as the length of boundary element (l_{be}), maximum center-to-center spacing of longitudinal bars that are laterally supported (h_x), center-to-center spacing of transverse reinforcement (s) and the total amount of transverse reinforcement in the boundary element (A_{sh}) in the x- and y-directions. Table 5.5 shows the comparison between the required and used amounts, and it can be concluded that, similar to Building #1, transverse reinforcement of the boundaries of the first-floor walls do not satisfy the SBE requirements of ACI 318-19 (shown in red).

Table 5.5 Assessment of transverse reinforcement of the wall boundaries

	Used	Required
l_{be} (in.)	16.54	6.29
h_x (in.)	9.21	6.04
s (in.)	3.94	3.02
$A_{sh\text{-}x}$ (in.^{2})	0.37	1.10
$A_{sh\text{-}y}$ (in.^{2})	0.24	0.48

Apart from the special boundary element provisions, transverse reinforcements of 2nd to 7th floor wall boundaries of Building #2 have to be checked if they must satisfy the ordinary boundary element (OBE) requirements. According to ACI 318-19 if the longitudinal reinforcement ratio (ρ) of the wall boundaries is higher than $400/f_y$, OBE requirements have to be satisfied. To this end, ρ is calculated for each wall and it is found that it is higher than $400/f_y$ at every floor. Figure 4.5 summarizes the required provisions and Table 5.6 shows the assessment which shows that similar to Building #1, wall boundaries do satisfy OBE requirements.

Table 5.6 Check on the OBE requirements

	Used	Required
l_{be} (in.)	16.54	6.29
h_x (in.)	6.91	14.00
s (in.)	3.94	5.98

Finally, story drift ratios in the wall direction are calculated and compared with ASCE 7-16 maximum drift ratio of 2% (Δ_a). Drift ratios given in Figure 5.3 represent the inelastic story drifts which are calculated by multiplying analysis results with C_d/I_e. A comparison between Figures 4.6 and 5.3 exhibits that maximum inter-story drift ratio which occurs at the 4th floor are almost the same for both of the structures with a value of 1.55%

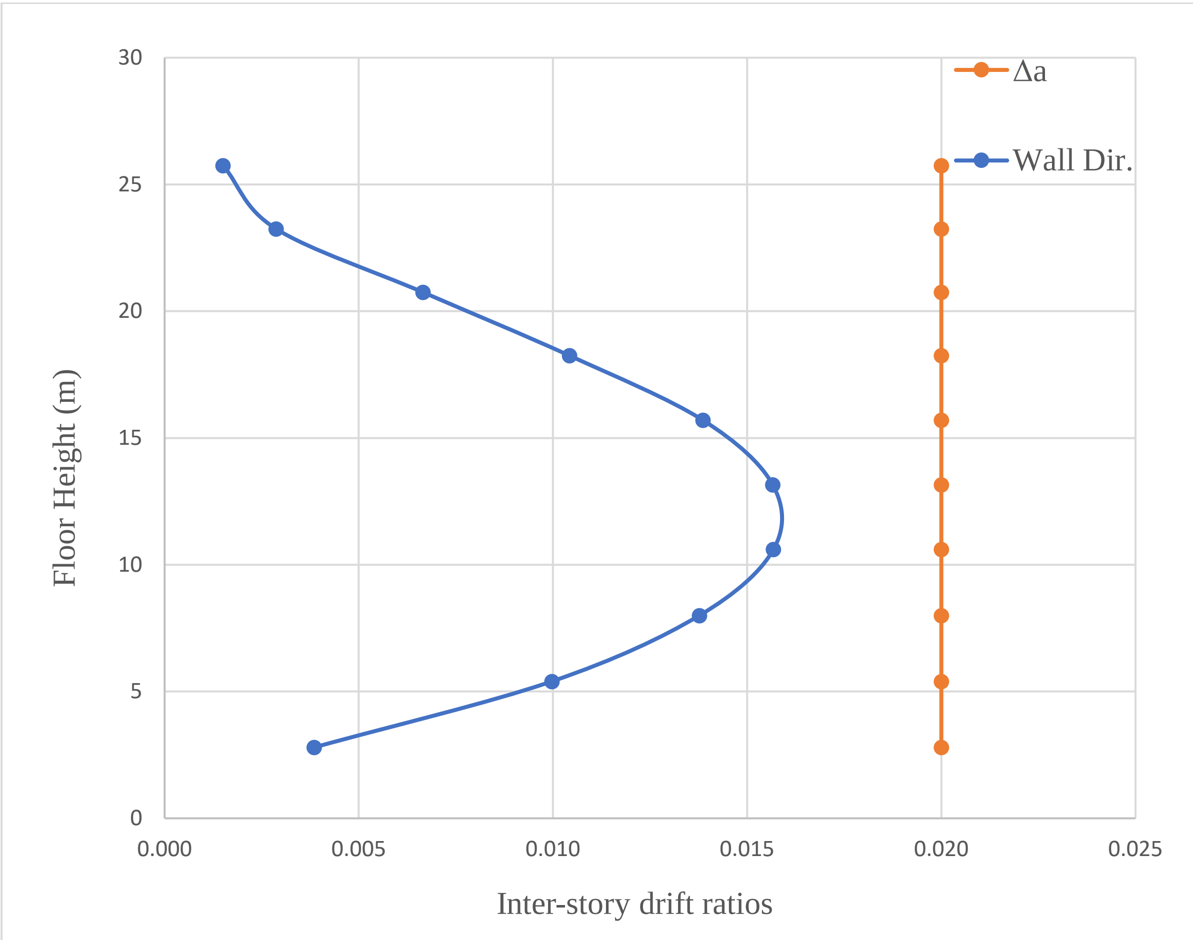

Figure 5.3 Inelastic story drift ratios in the wall direction

5.2 Columns

The lateral force resisting system of the test structure in the y-direction consists of 3 bay special reinforced concrete moment frames (R=8, Cd=5.5). Section sizes and the reinforcement details of the corner columns (C1) and the perimeter columns (C2) are given in Table 2.4, and Figures 2.7 and 2.8 respectively. Factored axial force-moment (ϕP-ϕM) capacity of the columns are calculated and compared with the demands that are calculated using the analysis procedure and loading conditions given in Chapter 3. This comparison is given in Figure 5.4 for the first floor C1 and C2 columns under different load combinations and it shows that the axial load and bending moment demands at the base of Building #2 columns do not exceed the ϕP_n-ϕM_n capacity. Although the same comparisons are done for the upper story columns and a similar behavior is observed (ϕP_n-$\phi M_n > P_u$-M_u), they are not included in this report.

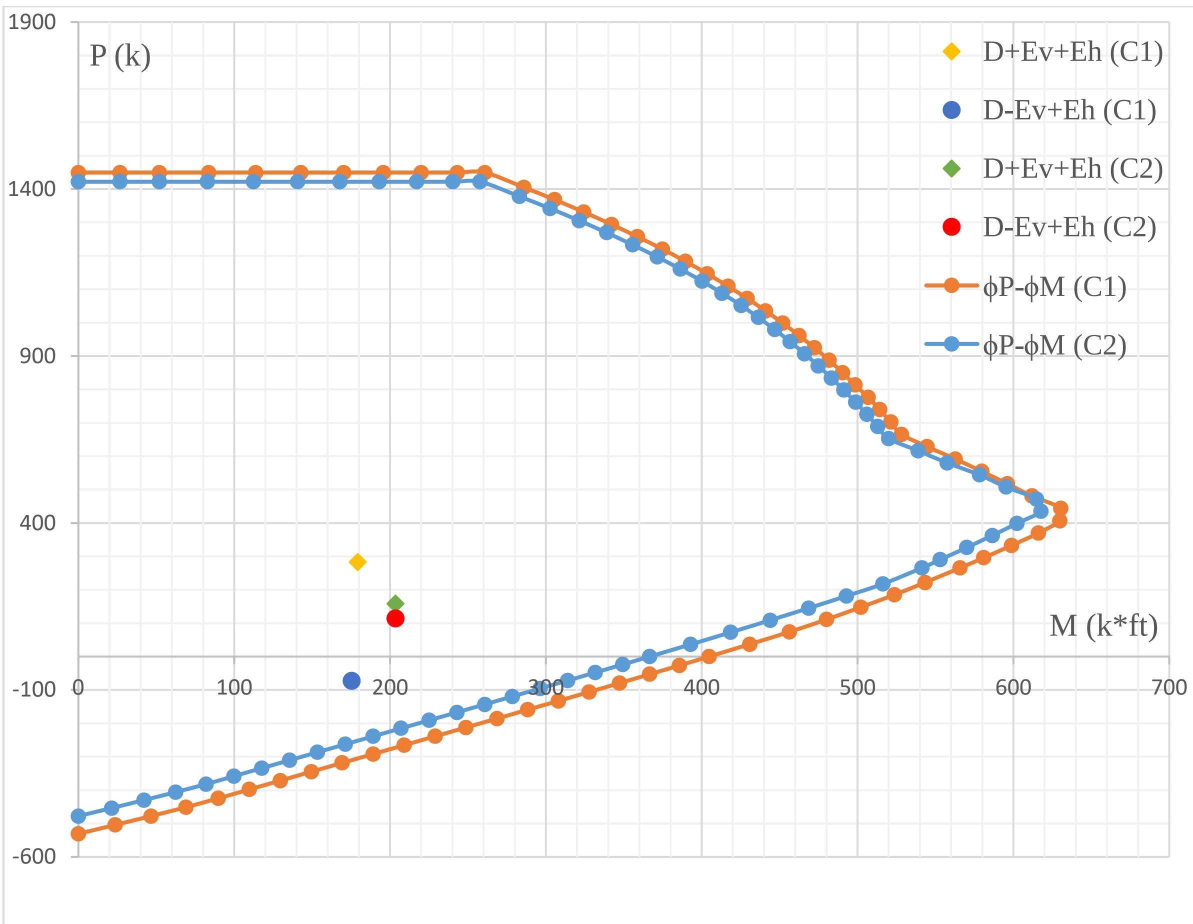

Figure 5.4 Factored integration diagram of C1 and C2 columns

Detailing requirements of the column transverse reinforcement defined by ACI 318-19 are given in Figure 4.8. Spacing provisions of the transverse reinforcement are given differently for three different locations along the column height. Spacing between the joint face and l_o away from it, and also the spacing at the lap splices are defined by s_1, and the spacing between the two is defined by s_2. Table 5.7 shows the required and the experimental values of s_1 and s_2 which yields that provided spacing of transverse reinforcement does satisfy the ACI 318 provisions.

Table 5.7 Spacing of transverse reinforcement of columns

		Provided (mm.)		Required (mm.)	
		s_1	s_2	s_1	s_2
Floor 1	C1-C2	60	100	132	132
Floor 2	C1-C2	60	100	125	132
3rd-4th-5th Floors	C1-C2	70	100	125	132
6th and 7th Floors	C1-C2	85	100	125	132
8th-9th-10th Floors	C1-C2	85	100	114	114

Similarly, the total cross-sectional area of the transverse reinforcement in x and y directions ($A_{sh,x}$ and $A_{sh,y}$), and the maximum center-to-center spacing of longitudinal bars that are laterally supported (h_x) are calculated and compared with the ACI 318 requirements in Tables 5.8 and 5.9 respectively.

Table 5.8 A_{sh} assessment of Building #2 columns

$A_{sh,x}$-$A_{sh,y}$		Provided (mm^2)	Required (mm^2)
Floors 1 and 2	C1-C2	471.2	349.8
3rd-4th-5th Floors	C1-C2		310.1
6th through 10th Floor	C1-C2		308.1

Table 5.9 h_x assessment of Building #2 columns

	Provided (mm)		Required (mm)
	C1	C2	
Floor 1	224.00	149.33	355.6
2nd- 10th Floors	265.33		

Calculations of shear strength (V_n) and the design shear force (V_e) of the columns were explained in detail in Chapter 4.2. Similar calculations are performed for the Building #2 columns and the demand to capacity ratios are given in Table 5.10 directly.

Table 5.10 Shear strength assessment of the Building #2 columns

$V_e / \phi V_n$		l_0	middle
Floor 1	C1	0.28	0.47
	C6	0.36	0.50
Floor 2	C1	0.33	0.65
	C6	0.46	0.64
Floor 3	C1	0.39	0.69
	C6	0.53	0.69
Floor 4	C1	0.37	0.64
	C6	0.48	0.63
Floor 5	C1	0.25	0.42
	C6	0.47	0.63
Floor 6	C1	0.28	0.40
	C6	0.51	0.69
Floor 7	C1	0.22	0.32
	C6	0.45	0.62
Floor 8	C1	0.17	0.24
	C6	0.36	0.50
Floor 9	C1	0.15	0.21
	C6	0.31	0.45
Floor 10	C1	0.13	0.19
	C6	0.24	0.34

Comparisons between Tables 4.9, 4.10, 4.11 and 4.14 with Tables 5.7, 5.8, 5.9 and 5.10 show that although the perimeter columns of Building #1 do not satisfy some of provisions of the ACI 318-19, with the improvements made on the transverse reinforcements, Building #2 columns satisfy all the provisions related with the shear strength and the transverse reinforcement detailing.

The inelastic inter-story drift ratios are also calculated in the moment frame direction and compared with the ASCE 7 maximum drift ratio limit of 2%. The comparison is given in Figure 5.5. Similar to the behavior of the buildings in the wall direction, the drift ratios of the two structures in the frame direction are also similar, increasing slightly from a maximum value of 0.7% to 0.8%.

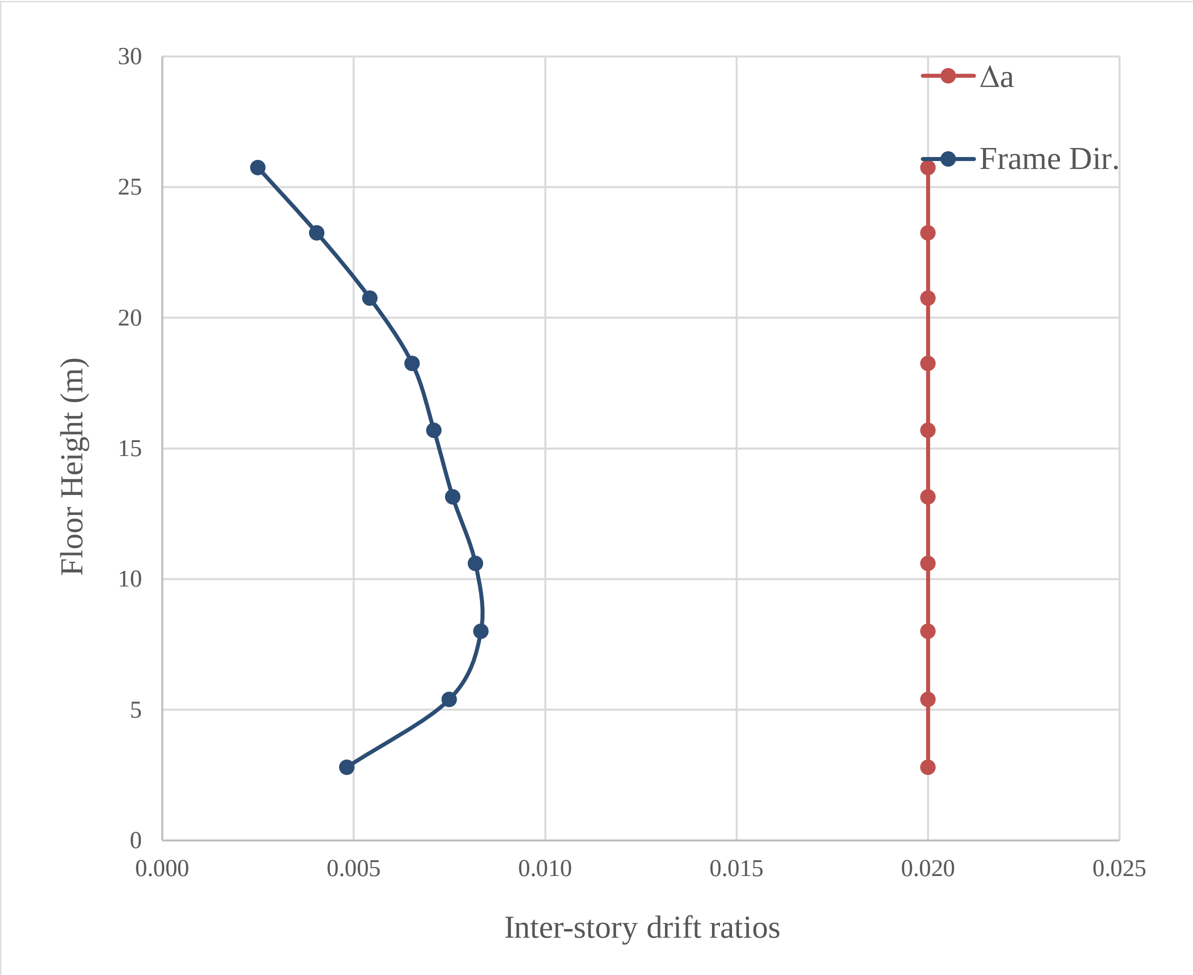

Figure 5.5 Building #2 story drift ratios in the moment frame direction

5.3 Beams

When the moment-frame beams of the Building #1 and Building #2 are compared, it is observed that the beams dimensions are smaller for the latter. While the amount of the longitudinal reinforcement at the ends of the beams stays mostly the same, more reinforcement is used at the center of the beams for the Building #2. Beam moment demand to capacity ratios are calculated at these three different locations (ends and the center) and given in Table 5.11. For the calculation of the factored moment capacity, T-beam configurations are assumed and the slab reinforcement at the effective overhanging flanges are included in the calculations.

Table 5.11 Moment capacity assessment of the perimeter beams

$M_u/\phi M_n$		G1/G3			G2	
		Outer	Center	Inner	Ends	Center
2nd Floor	+	0.69	0.22	0.84	0.66	0.17
	-	0.80	0.16	0.93	0.76	0.11
3rd Floor	+	0.74	0.23	0.77	0.63	0.18
	-	0.86	0.18	0.98	0.81	0.13
4th Floor	+	0.73	0.22	0.85	0.64	0.16
	-	0.94	0.17	0.96	0.72	0.11
5th Floor	+	0.78	0.20	0.82	0.61	0.15
	-	0.89	0.16	1.05	0.69	0.10
6th Floor	+	0.70	0.26	0.86	0.58	0.20
	-	0.87	0.14	1.02	0.72	0.10
7th Floor	+	0.72	0.20	0.72	0.62	0.17
	-	0.85	0.13	0.85	0.70	0.09
8th Floor	+	0.71	0.21	0.71	0.57	0.19
	-	0.82	0.10	0.82	0.77	0.09
9th Floor	+	0.51	0.16	0.51	0.55	0.16
	-	0.78	0.06	0.78	0.60	0.06
10th Floor	+	0.34	0.16	0.34	0.48	0.18
	-	0.48	0.00	0.48	0.54	0.01
Roof	+	0.14	0.13	0.14	0.23	0.13
	-	0.23	0.02	0.23	0.31	0.01

It can be observed from the comparison of Tables 4.15 and 5.11 that the beams of the Building #2, like Building #1, satisfy the ACI 318 flexural strength requirement with exceptions of 5th and 6th floors G1-G3 beams' inner ends where the demand to capacity ratios are bigger than 1.0.

The strong column-weak beam requirement of the ACI 318, $\frac{\sum M_{nc}^{top} + M_{nc}^{bottom}}{\sum M_{nb}^{+} + M_{nb}^{-}} \geq 1.2$, is also checked for the Building #2 beams. Table 5.12 shows the ratio of the total moment capacity of the columns framing into a joint to total moment capacity of the beams framing into the same joint under the two different load combinations and for the sway of the building in +Y and -Y directions separately. Comparison with Table 4.16 shows that with the improved detailing of the Building #2 columns, the ratio has higher values. While the Building #1 has a ratio as low as 1.14 at the 3rd floor Joint 2, the lowest value for the Building #2 is 1.81 at the same joint.

Table 5.12 Strong Column-Weak Beam assessment of the Building #2

$\frac{\sum Mnc}{\sum Mnb}$	Joint 1				Joint 2			
	$D + E_v + E_h$		$D - E_v + E_h$		$D + E_v + E_h$		$D - E_v + E_h$	
	Sway +Y	Sway -Y	Sway +Y	Sway -Y	Sway +Y	Sway -Y	Sway +Y	Sway -Y
Floor 2	2.38	3.55	2.26	3.46	2.36	2.37	2.24	2.26
Floor 3	2.05	2.97	1.95	2.89	1.90	1.92	1.81	1.83
Floor 4	2.06	3.00	1.97	2.92	1.95	1.98	1.86	1.89
Floor 5	-	-	-	-	1.98	1.99	1.90	1.91
Floor 6	-	-	-	-	2.16	2.26	2.09	2.19
Floor 7	-	-	-	-	2.23	2.27	2.16	2.20
Floor 8	-	-	-	-	2.56	2.94	2.50	2.86
Floor 9	-	-	-	-	3.16	2.90	3.09	2.85
Floor 10	-	-	-	-	3.92	3.95	3.87	3.91

The detailing requirements of the transverse reinforcement of the beams was given in Figure 4.10. Comparison between the required and provided spacing of the transverse reinforcement of the beams showed that, unlike Building #1, up until the 8th floor the spacing provisions were satisfied. However, above the 8th floor, spacing along $2h_b$ away from the joint faces and along the lab splices are higher than the maximum required values. These findings are summarized in Table 5.13.

Table 5.13 Transverse reinforcement spacing assessment of the perimeter beams

		Provided (mm)		Required (mm)		
		along $2h_b$	middle/lab splice	along $2h_b$	middle	at lab splice
Story 2	G1/G3	100.0	100.0	106.0	212.0	100.0
	G2	100.0	100.0	106.0	212.0	100.0
Story 3	G1/G3	100.0	100.0	106.0	212.0	100.0
	G2	100.0	100.0	106.0	212.0	100.0
Story 4	G1/G3	100.0	100.0	106.0	212.0	100.0
	G2	100.0	100.0	106.0	212.0	100.0
Story 5	G1/G3	100.0	100.0	106.0	212.0	100.0
	G2	100.0	100.0	106.0	212.0	100.0
Story 6	G1/G3	100.0	100.0	106.4	212.8	100.0
	G2	100.0	100.0	106.4	212.8	100.0
Story 7	G1/G3	100.0	100.0	106.4	212.8	100.0
	G2	100.0	125.0	106.4	212.8	100.0
Story 8	G1/G3	100.0	200.0	93.9	187.8	93.9
	G2	100.0	200.0	93.9	187.8	93.9
Story 9	G1/G3	100.0	200.0	93.9	187.8	93.9
	G2	100.0	200.0	93.9	187.8	93.9
Story 10	G1/G3	100.0	200.0	93.9	187.8	93.9
	G2	100.0	200.0	93.9	187.8	93.9
Roof	G1/G3	100.0	200.0	93.9	187.8	93.9
	G2	100.0	200.0	93.9	187.8	93.9

Calculations of the shear strength (ϕV_n) and the design shear forces (V_e) of the beams were explained in Section 4.3 in detail. Similar calculations yielded the results that are shown in Table 5.14. Comparison with Table 4.20 shows that although the changes made in the beam design resulted in satisfaction of the shear strength requirements for the 9th, 10th floors and the roof, for the floors below, factored shear strength along 2hb away from the joint faces are still lower than the ACI 318-19 requirement.

Table 5.14 Beam shear strength assessment

$V_e/\phi V_n$ (kip)		G1/G3	G2
2nd Floor	along $2h_b$	1.73	1.60
	mid-span	0.71	0.64
3rd Floor	along $2h_b$	1.79	1.68
	mid-span	0.78	0.72
4th Floor	along $2h_b$	1.65	1.54
	mid-span	0.73	0.67
5th Floor	along $2h_b$	1.52	1.54
	mid-span	0.66	0.67
6th Floor	along $2h_b$	1.40	1.47
	mid-span	0.49	0.54
7th Floor	along $2h_b$	1.23	1.23
	mid-span	0.51	0.59
8th Floor	along $2h_b$	1.06	1.29
	mid-span	0.58	0.80
9th Floor	along $2h_b$	0.96	1.05
	mid-span	0.50	0.59
10th Floor	along $2h_b$	0.87	0.87
	mid-span	0.40	0.40
Roof	along $2h_b$	0.84	0.84
	mid-span	0.48	0.48

5.4 Beam-Column Joints

As noted earlier, some of the joints of Building #1 failed during the experiments conducted in 2015. Therefore, one of the biggest alterations made to design of Building #2 structural elements was to increase the shear strength of the joints. To this end, the spacing of the transverse reinforcement in the joint zone was decreased to 60 mm for the second and the third floors, to 70 mm at 4th and 5th stories and to 85 mm for the floors 6th through roof. Also, the number of stirrup legs increased to 6 from 2. At the end of the 2018 experiments, no joint failure was observed.

As explained in Section 4.4, for the calculations of the beam-column joint shear strength three different methods are used; the method required by ASCE 41-17 and the methods proposed by LaFave and Kim [5], and Hassan [3]. Same approaches are also used for the calculation of the shear strength of Building #2 joints. The details of the calculations e.g., used parameters, effective joint area, are explained in detail in Section 4.4. Therefore, in this section, only the results are provided directly for all the three methods. Table 5.15 shows the joint shear demand over capacity ratios, and all the three methods suggested that the joints of Building #2 should be safe without any damage under shear.

Table 5.15 Joint shear strength assessments based on ASCE 41-17, LaFave and Kim [5] and Hassan [3]

	ASCE 41-17		LaFave and Kim		Hassan	
Vu/ϕVn	Joint 1	Joint 2	Joint 1	Joint 2	Joint 1	Joint 2
Story 2	0.55	0.60	0.54	0.62	0.70	0.76
Story 3	0.61	0.74	0.59	0.74	0.77	0.93
Story 4	0.63	0.79	0.60	0.78	0.77	0.96
Story 5	0.55	0.79	0.62	0.78	0.67	0.96
Story 6	0.49	0.65	0.59	0.68	0.61	0.81
Story 7	0.45	0.64	0.55	0.69	0.56	0.80
Story 8	0.36	0.57	0.45	0.61	0.45	0.72
Story 9	0.27	0.50	0.36	0.56	0.34	0.67
Story 10	0.26	0.35	0.37	0.43	0.35	0.46
Roof	0.29	0.48	0.47	0.78	0.38	0.64

CHAPTER 6. SENSITIVITY STUDIES

As mentioned in Chapter 3, the idea behind the chosen modeling approaches was to create elastic models that will represent the structures' behavior as close as possible to the experimental behavior. To this end, first, since the boundaries of the walls were designed as columns, two different models were created; one to represent the wall direction behavior of the buildings so the walls were modelled as shell element, and the other one to represent the frame direction behavior with line elements at the boundaries (to represent the columns) and shell elements at the middle (to represent the walls). Figures 3.1 and 3.2 show the plan and elevation view of these different models respectively. Secondly, knowing that the buildings' seismic force resisting systems (SFRS) do not comply with the requirements of the ASCE 7-16 to be called as dual systems and therefore the SFRS in the wall direction is special RC shear walls, in the ETABS models the beams that connect the perimeter frames to the shear walls, e.g., G7 and G9 beams (see Figure 2.2), were not modelled. This chapter focuses on some sensitivity studies conducted to understand the effects of these different modeling approaches.

6.1 Wall model versus Frame model

The following comparisons are intended to show the influence of two different wall models on the behavior of the building(s) (see Figure 3.1a and Figure 3.1b). The resulting differences are compared for both Building #1 and Building #2 in terms of the building periods, walls' and perimeter columns' P-M couple results, and the story drift ratios in the wall and frame directions.

Table 6.1 Comparison of the structure periods for different models

T (s.)	Wall Dir.		Frame Dir.	
	Wall model	Frame model	Wall model	Frame model
Building #1	1.06	1.08	0.7	0.71
Building #2	1.14	1.17	0.72	0.73

As shown in Table 6.1, different models yielded in slightly different periods, i.e., a difference of 0.02 and 0.03 seconds in the wall direction for Building #1 and Building #2 respectively, and 0.01 seconds in the frame direction for both of the structures. Figures 6.1 and 6.2 show the axial load-moment demands for the first story walls resulting from the two different models respectively for Building #1 and Building #2. Both figures indicate a similar behavior, modeling the wall boundaries as columns (line elements) instead of shell elements only slightly decreases the moments that are taken by the walls while keeping the axial loads at the same level. Demands are presented with ϕP-ϕM capacity diagrams to show that for both of the models resulting forces are smaller than the capacity of the walls in terms of the axial load and moment.

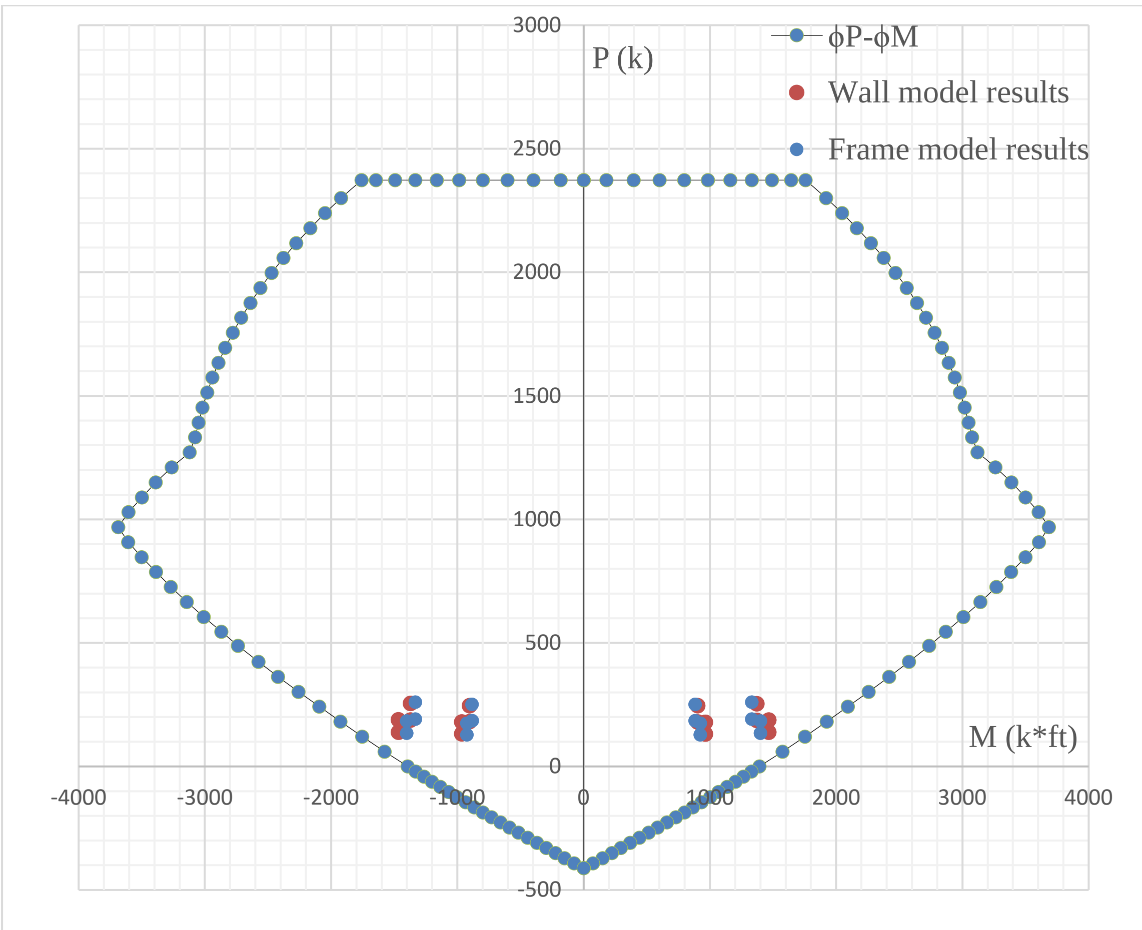

Figure 6.1 Comparison of P-M forces of the first story walls for Building #1

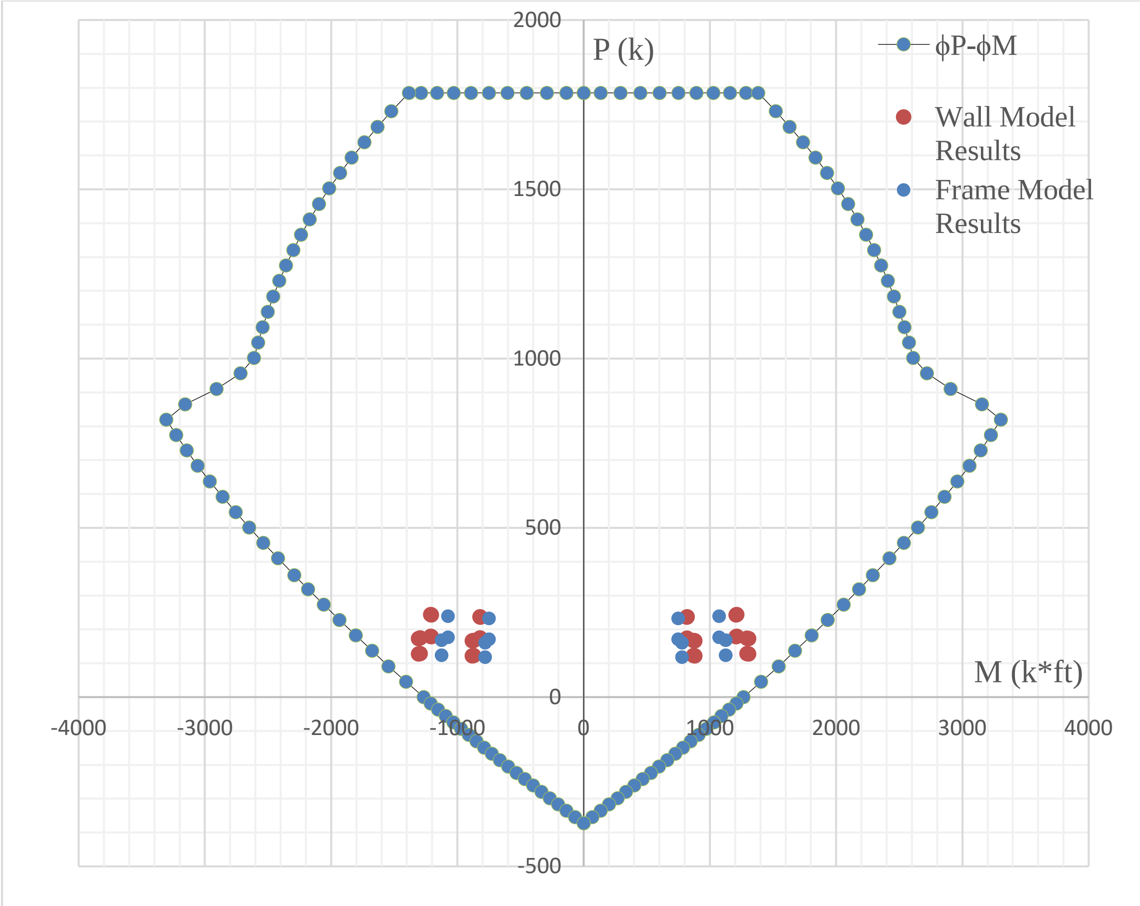

Figure 6.2 Comparison of P-M forces of the first story walls for Building #2

Similarly, P and M values that are carried by the corner and the perimeter columns (C1 and C2 columns) are also compared for the two different models in the frame direction. To illustrate, results from only the C1 columns are given in Table 6.2 for both structures. The table concludes that not only the loads carried by the walls but also the ones taken by the columns do not differ much for the different models. Similar behavior is observed for the perimeter columns (C2).

Table 6.2 Comparison of the column load results

Corner Columns	Frame Model		Wall Model	
	P_{max} (kip)	M_{max} (kip-ft)	P_{max} (kip)	M_{max} (kip-ft)
Building #1	296	175	315	180
Building #2	283	180	292	178

The effect of the different modeling types of wall boundary elements on the analysis results are also checked by comparing the inter-story drift ratios of the two different buildings in the wall and the frame directions. Like the structure periods and the P-M demands, different models resulted in slightly different drift ratios for both buildings. Results are shown and compared in Figures 6.3 and 6.4. For Building #1, while the wall model resulting in a 1.55% drift ratio at the 5th floor, frame model gave almost the same value, 1.54%, at the same floor in the wall direction. The difference of 0.01% for the first structure increased to 0.06% for the second structure. In the frame direction, similar to the wall direction, results from the two different models are more similar for Building #1 than Building #2. A maximum difference of 0.08% occurs at the 3rd floor of Building #2. In general, due to very slight discrepancies between the models, analysis results are thought to be accurate and meaningful.

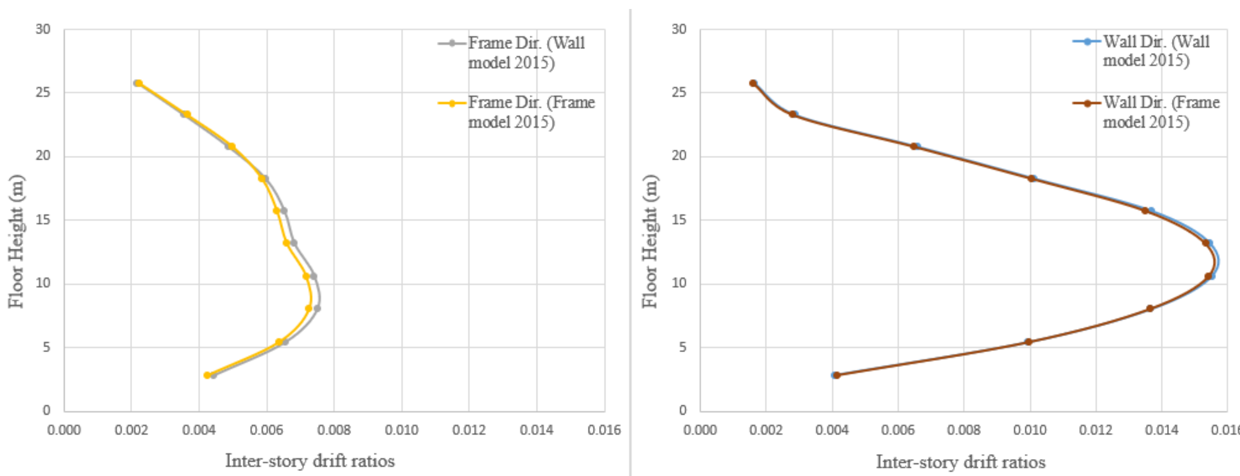

Figure 6.3 Inter-story Drift Ratios in the Frame Dir. (left) and Wall Dir. (right) for Building #1

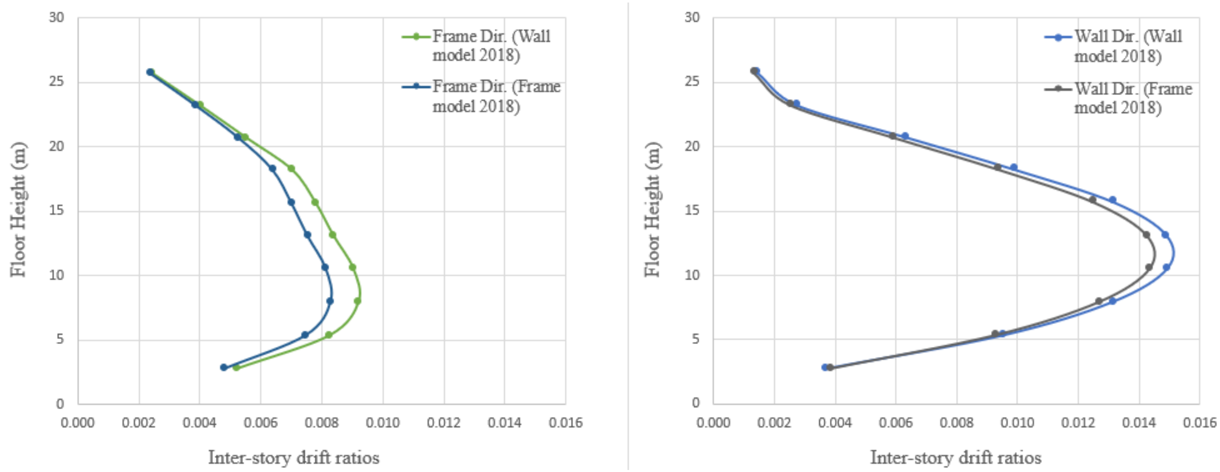

Figure 6.4 Inter-story Drift Ratios in the Frame Dir. (left) and Wall Dir. (right) for Building #2

6.2 Effect of Modeling G7 and G9 Beams

Different models that include the G7 and G9 beams were created for each structure to be able to see the effects of modeling the beams that connect the walls to the perimeter moment frames. According to ASCE 7-16 §12.2.3.3, where different seismic force-resisting systems are used in combination to resist seismic forces in the same direction, the value of the response modification coefficient (R) shall not be greater than the least value of R for any systems used in that direction. Also, the deflection amplification factor (C_d) and the overstrength factor (Ω_0) should be consistent with R required. Therefore, based on ASCE 7-16 Table 12.2-1, the R is kept as 5 for the new models. It should be noted here that similar to the previous models, the weights of the buildings are adjusted by adding distributed gravity loads to the floors to be able to keep the total mass of the buildings and story masses the same with the reported values from the experiments. Analysis results for the two different models are compared only in the wall direction since the alterations to the models are only made in the wall direction. Figure 6.5 illustrates the new and previously used models.

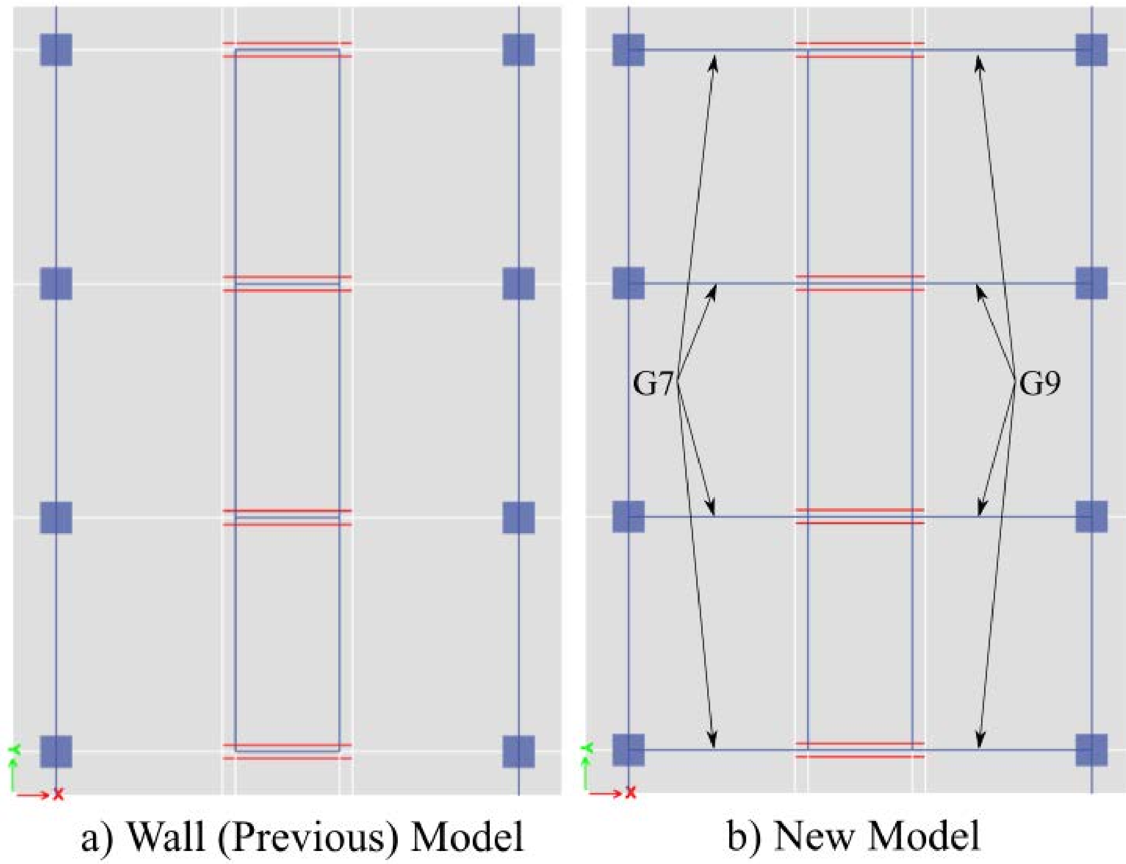

Figure 6.5 Comparison of the models

Results are first compared in terms of the structural periods. Table 6.3 shows the periods of the buildings in the wall direction for the previously used wall model and for the new model. As expected, connecting the walls to the perimeter columns with beams as deep as 470 mm (450 mm for Building #2) affected the periods of the buildings extensively, 53% and 62% reductions for the Building #1 and Building #2 natural periods respectively.

Table 6.3 Structure Periods in the Wall Direction of the Two Models

T (s.)	Wall Model	New Model
Building #1	1.06	0.5
Building #2	1.14	0.44

Apart from the building periods, demands on the walls are also checked again to be able to see if they exceed the ACI 318-19 capacity formulations. To this end, first, walls factored nominal axial load-moment capacities (ϕP-ϕM) are compared with the P_u-M_u at every story for both of the buildings. Figures 6.6 and 6.7 show the comparison for the first story walls for the two different buildings respectively. A similar behavior was observed for both of the buildings, the new models resulted in lower moment and axial load demands. Lower moment values can be explained by the moments carried by the moment frames in the wall direction. Axial load demands decreased 15% to 25% due to the effect of beam shear forces.

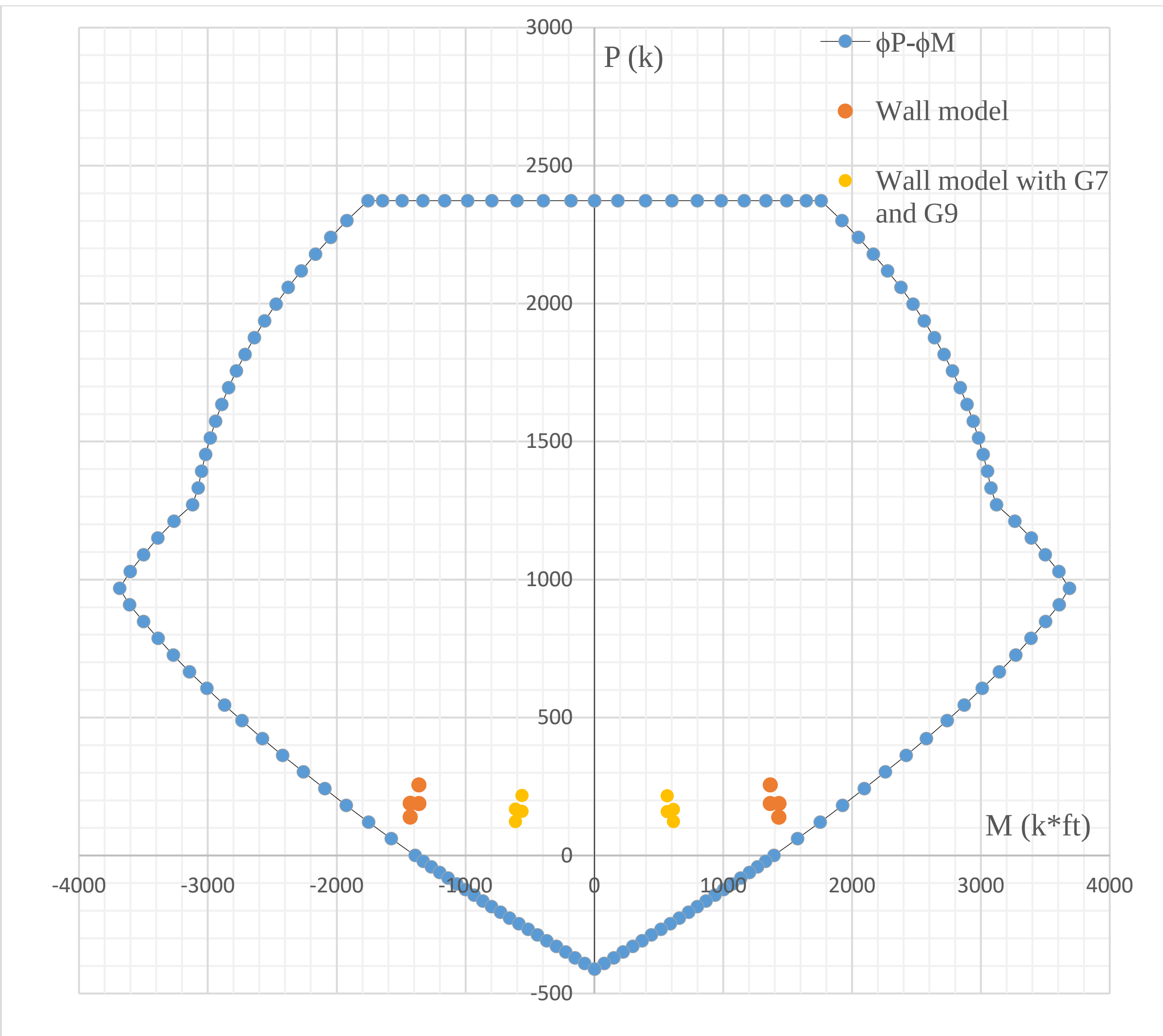

Figure 6.6 Comparison of First Floor Wall P-M Demands for Building #1

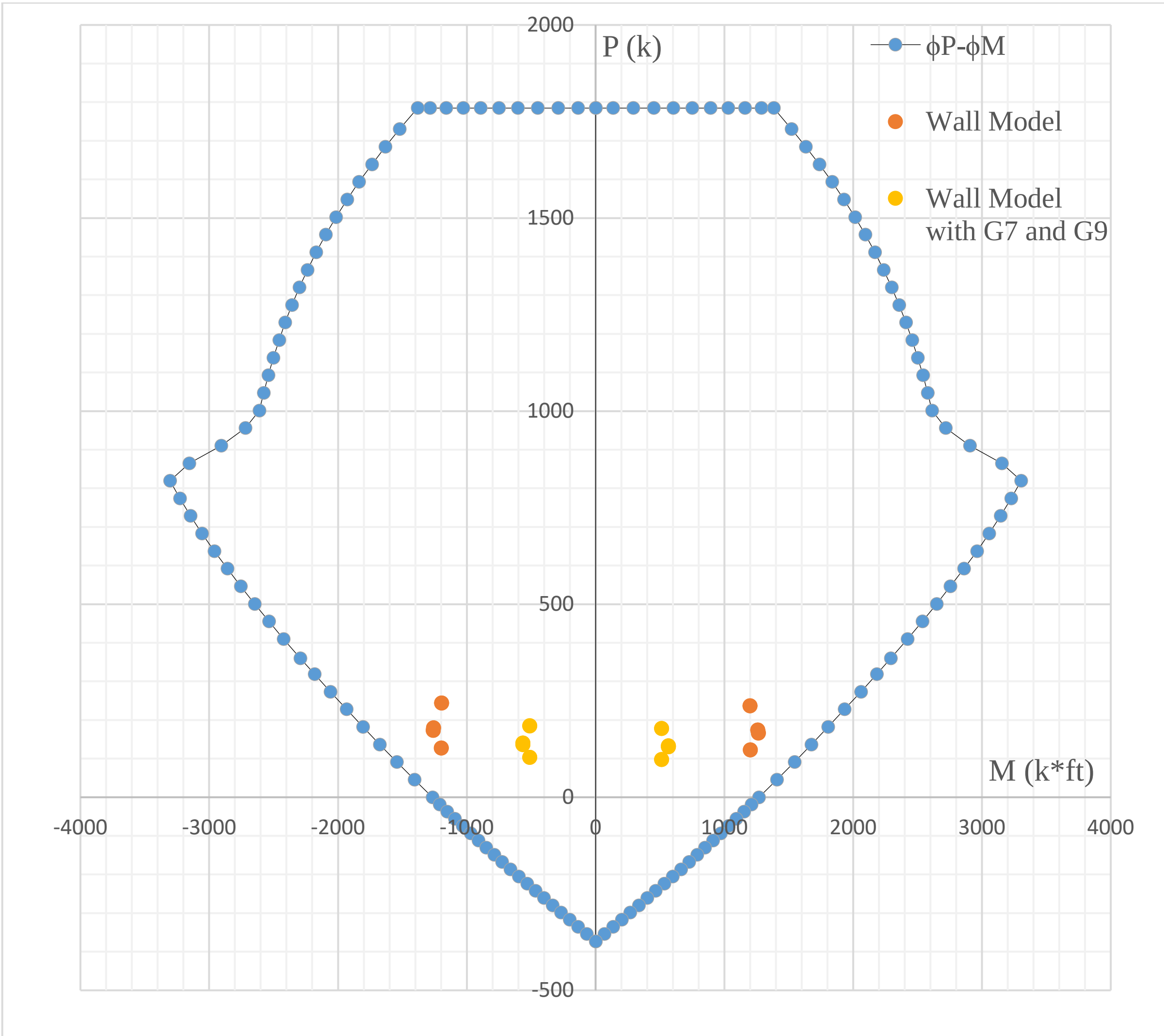

Figure 6.7 Comparison of First Floor Wall P-M Demands for Building #2

Wall design shear forces (V_e) are recalculated for the new models based on equations 4.2 and 4.3 and compared with the shear forces from the previous models in Figures 6.8 and 6.9 for Building #1 and Building #2, respectively. Figures illustrate the change of V_e over the wall height, and it can be observed that both of the models resulted in a similar behavior, decreasing wall shear forces with increasing height except the second and the seventh floors where the walls are terminated, for both of the buildings. Although the periods of the structures decreased substantially due to the shape of the response spectrum, base shears of the structures did not increase at same rate. Comparing the shear forces carried by the walls for Building #1 and

Building #2 shows that while the new model resulted in lower forces for the former, except the first floor, for the latter it increased the forces by approximately 35%.

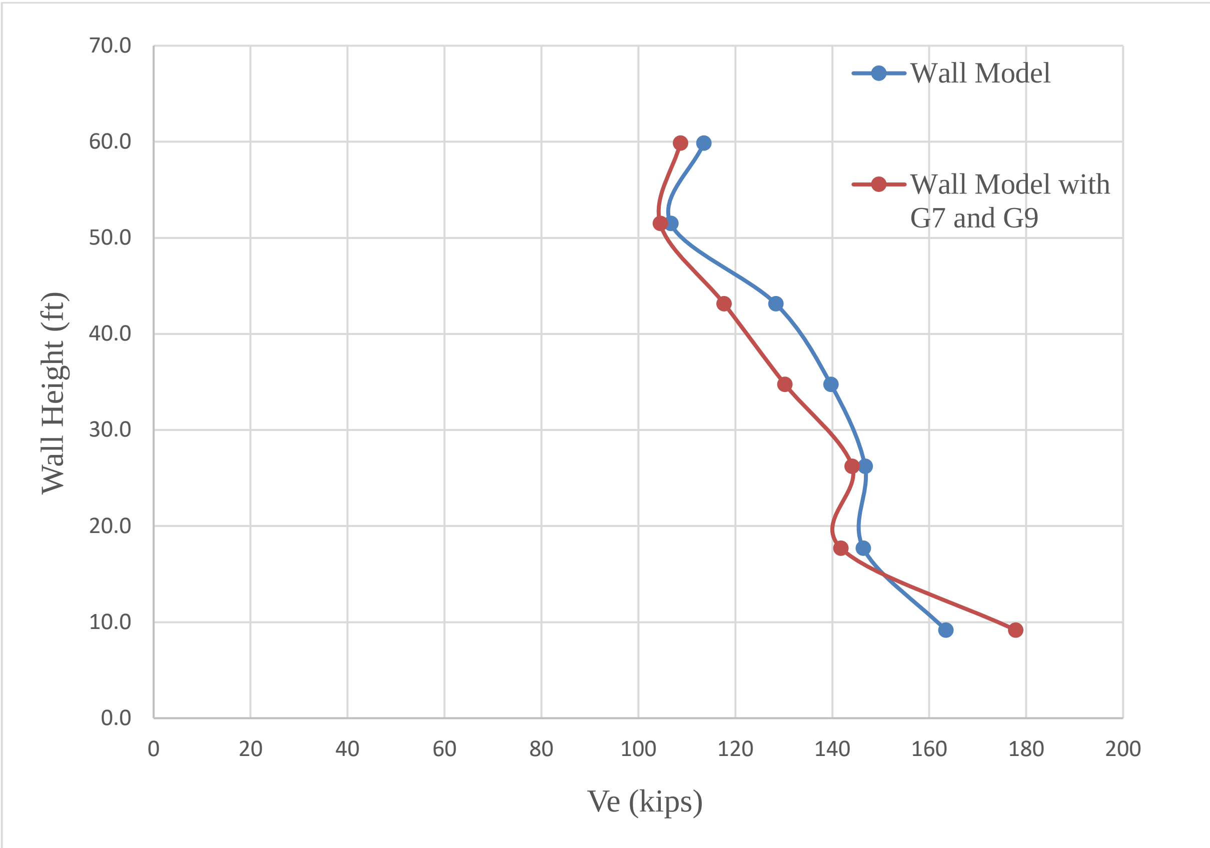

Figure 6.8 Old model versus New model for Building #1

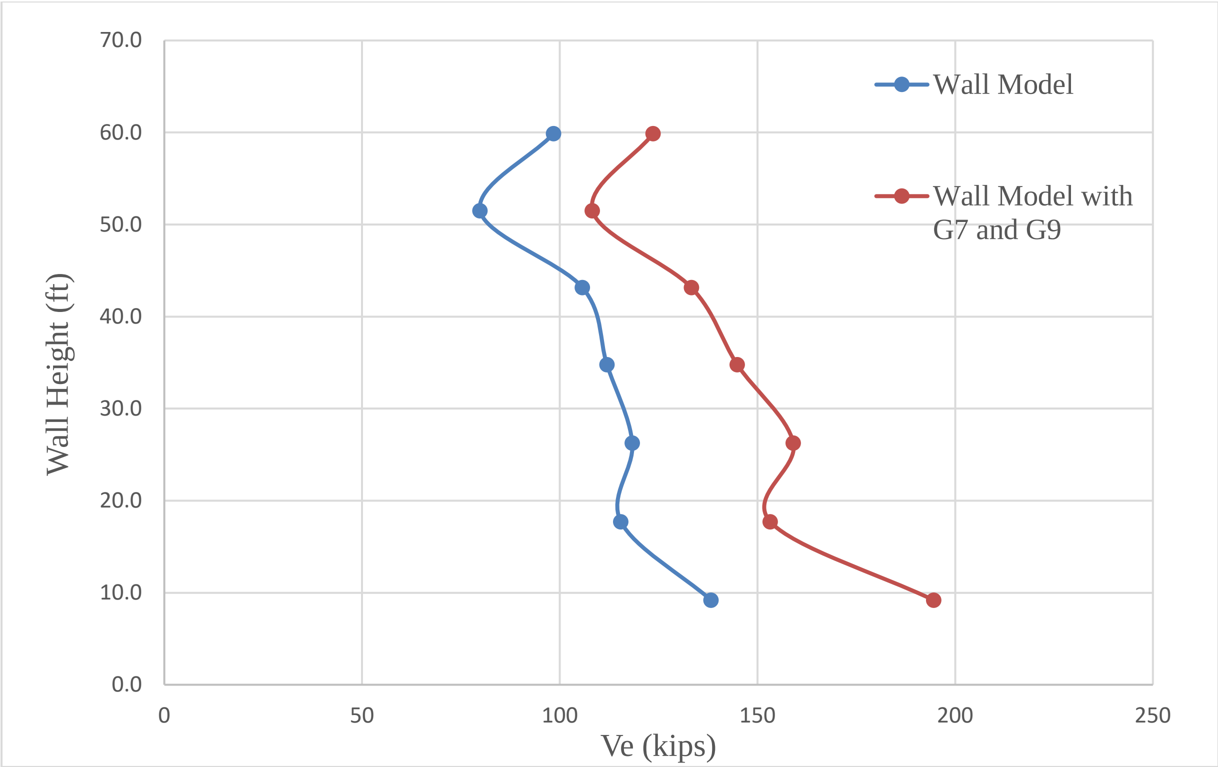

Figure 6.9 Old model versus New model for Building #2

The design shear forces are also compared with the shear strength of the walls in Table 6.4. Although the new models suggest the shear failure of the walls for Building #2 at the 3rd, 4th, 5th and 7th floors, knowing that during the experiments, walls did not fail under shear would show that the original modeling idea (models without G7 and G9 beams) was logical and gives better estimates of the demands within the limits of linear elastic analysis.

Table 6.4 Wall Shear Forces to Strength Ratio for the New Model

Ve/ϕVn	Building #1	Building #2
F1	0.71	0.97
F2	0.67	0.93
F3	0.72	1.28
F4	0.65	1.16
F5	0.59	1.07
F6	0.54	0.91
F7	0.79	1.26

CHAPTER 7. CONCLUSIONS

This chapter provides some concluding remarks of the assessment of 2015 and 2018/2019 E-Defense 10-story reinforced concrete buildings based on the latest provisions of ACI 318 [1] and ASCE 7 [2]. Different models, to represent the behavior of the buildings in the wall and frame directions, were created for both of the buildings using the structural analysis software ETABS. For the creation of the models, actual floor dimensions, member sizes, and material strengths were used based on the information provided by the Japanese researchers. Modal response spectrum analysis was used to determine element demands in accordance with the provisions of ASCE 7-16 §12.9.1. Similarly, the response modification factor (R) and the deflection amplification factor (C_d) were selected based on ASCE 7-16 Table 12.2-1. The applied response spectrum was created based on the assumption of considering the JMA Kobe scaled to 100% as the ASCE 7's Risk-Targeted Maximum Considered Earthquake (MCE_R). To this end, spectral acceleration values were multiplied by 2/3 at every period (T) to obtain the Design Response Spectrum. Analysis results were then compared with the ACI 318-19 capacity formulations for the structural walls, moment-frame columns and beams at every story.

For the 2015 test structure walls, the requirements given in ACI 318-19 Section 18.10, such as the P-M couple forces, reinforcement requirements, shear strength, special and ordinary boundary element provisions, were checked. Amongst these requirements, the major item that was not satisfied with the detailing requirement for transverse reinforcement of the special boundary elements for the first story wall boundaries. Table 4.6 shows that while the center to center spacing of the transverse reinforcement was higher than the maximum requirement, its total amount was less than the minimum set value ($A_{sh,min}$) both in the x- and y- directions. However, given the low drift demands expected under DE and even MCE_R level demands, it is expected that the provided detailing is sufficient to avoid any significant wall damage in these events. In terms of the structure's perimeter columns (C1 and C2 columns), similar to the structural walls, longitudinal reinforcement requirements were satisfied while transverse reinforcement detailing requirements were not satisfied. Also, unlike the walls, shear strength was less than the required value along l_o away from the joint faces for the floors 5 and above. Similarly, the spacing of the transverse reinforcement along $2h_b$ away from the joint faces and at the lap splices were higher than the minimum requirement for the perimeter beams (G1, G2 and G3) of the 5th floor through roof. Although the shear strength was higher than the design shear forces at the mid-section of the beams, it was less along $2h_b$ away from the joint faces at every story. Another significant requirement of ACI 318 on the frame design is the strong column – weak beam connection which states that the sum of the nominal flexural strength of columns ($\sum M_{nc}$) framing into a joint must be 20% higher than the sum of the nominal flexural strength of the beams ($\sum M_{nb}$) framing into the same joint. Investigations on the 2015 structure beam-column joints showed that 3rd and 7th floor joints where the G1/G3 and G2 beams connecting to (Joint 2 of Table 4.16) and the 4th floor joint where CG1 and G1/G3 beams connected to (Joint 1 of Table 4.16) did not satisfy this requirement. The failures observed in Joint 2, at the 3rd, 4th and 5th floors, after the experiments conducted in 2015 led to an increased attention to the calculation of shear strength of beam-column joints. To this end, different approaches were used, starting with the shear strength formulation of ASCE 41-17. Based on Table 4.22, it was shown that current provisions of ASCE 41 (or ACI 318 since they both use the same formulation) were not able to predict these failures. However, usage of more detailed approaches developed by LaFave and Kim [5], and Hassan [3] suggested the joint shear failures at the floors where the damage was observed.

For the 2018/2019 test structure, main changes made on the structural element designs were focused on the shear design and transverse reinforcement detailing of the columns and the joints. To this end, joint zones and the columns sections, h_c away from the joint faces, were more heavily reinforced. Therefore, the perimeter columns and joints satisfied all the requirements of ACI 318-19. However, the spacing and the total amount of the transverse reinforcement used at the special boundary elements of the structural walls and some sections of the perimeter beams, $2h_b$ away from the joint faces, still did not satisfy the requirements. Also, shear strength of the perimeter beams up to the 9th floor were still less than the design shear forces. Unlike the 2015 test structure, the shear strength of the walls of the 2018/2019 test structures at the 7th floor did not satisfy the ACI 318-19 requirements. Finally, the story drifts were calculated and compared with the allowable story drift ratios (Δ_a) of ASCE 7 in the wall and frame directions separately. Results indicated a maximum value of 1.6% in the wall direction and at the 5th floor of 2015 test structure which is smaller than Δ_a=2%.

REFERENCES

[1] ACI (2019): 318-19 Building Code Requirements for Structural Concrete and Commentary American Concrete Institute.

[2] ASCE 7-16: Minimum Design Loads and Associated Criteria for Buildings and Other Structures. American Society of Civil Engineers, 2017.

[3] Hassan W. M. "Analytical and Experimental Assessment of Seismic Vulnerability of Beam-Column Joints without Transverse Reinforcement in Concrete Buildings". PhD dissertation, University of California, Berkeley, 2011.

[4] Kajiwara K., Tosauchi Y., Sato E., et al: "2015 Three-dimensional Shaking Table Test of a 10-story Reinforced Concrete Building on the E-Defense, Part1: Overview and Specimen Design of the Base Slip and Base Fixed Tests". 16th World Conference on Earthquake, 16WCEE 4012 (2017).

[5] LaFave J. M., and Kim J.-H. (2011). "Joint Shear Behavior Prediction for RC Beam-Column Connections." *International Journal of Concrete Structures and Materials*, International Journal of Concrete Structures and Materials, Korea Concrete Institute, 5(1), 57–64.

[6] Moehle Jack P., Ghodsi Tony, Hooper, John D., Fields, David C., and Gedhada, Rajnikanth (2011). "Seismic design of cast-in-place concrete special structural walls and coupling beams: A guide for practicing engineers," NEHRP Seismic Design Technical Brief No. 6, produced by the NEHRP Consultants Joint Venture, a partnership of the Applied Technology Council and the Consortium of Universities for Research in Earthquake Engineering, for the National Institute of Standards and Technology, Gaithersburg, MD, NIST GCR 11-917-11REV-1.

[7] Nakashima M., Nagae T., Enokida R., et al.: "Experiences, accomplishments, lessons, and challenges of E-Defense, Tests using world's largest shaking table". Japan Architectural Review 1.1 (Jan. 2018), pp. 4-17.

[8] NIST (2016). Seismic design of reinforced concrete special moment frames: A guide for practicing engineers, Second Edition, GCR 16-917-40, NEHRP Seismic Design Technical Brief No. 1, produced by the Applied Technology Council and the Consortium of Universities for Research in Earthquake Engineering for the National Institute of Standards and Technology, Gaithersburg, MD.

[9] Sato E., Tosauchi Y., Fukuyama K., et al.: "2015 Three-dimensional Shaking Table Test of a 10-story Reinforced Concrete Building on the E-Defense, Part2: Specimen Fabrication and Construction, Test Procedure, and Instrumentation Program". 16th World Conference on Earthquake, 16WCEE 4007 (2017).

[10] Seismic Evaluation and Retrofit of Existing Buildings: ASCE/SEI, 41-17 American Society of Civil Engineers, 2017.

[11] Tosauchi Y., Sato E., Fukuyama K., et al.: "2015 Three-dimensional Shaking Table Test of a 10-story Reinforced Concrete Building on the E-Defense, Part3: Base Slip and Base Fixed Test Results". 16th World Conference on Earthquake, 16WCEE 4016 (2017).